Material sources of the Roman brick-making industry in the I and II century A.D. from *IX*, *XI* and *Alpes Cottiae Regiones*

R. Scalenghe[1,4], F. Barello[2], F. Saiano[1,*], E. Ferrara[3], C. Fontaine[4], L. Caner[4], E. Olivetti[3], I. Boni[5] S. Petit[4]

[1]SAF, Università degli Studi di Palermo, Palermo, IT E.U.

[2]Soprintendenza per i Beni Archeologici del Piemonte e del Museo Antichità Egizie, Torino, IT E.U.

[3]Istituto Nazionale di Ricerca Metrologica, Torino, IT E.U.

[4]Université de Poitiers, UMR 7285 IC2MP HydrASA, Poitiers, FR E.U.

[5]Istituto per le Piante da Legno e l'Ambiente, Torino, IT E.U.

(*) Corresponding author' Email: filippo.saiano@unipa.it

Abstract Bricks, fine pottery, ceramic gears and tiles are among the man-made objects routinely recovered in archaeological documentation. Sites associated with early civilizations can provide thousands of samples from a single excavation. They come in endless varieties according to economic and social circumstances and, even as debris can last almost forever providing important clues about the past behaviours in human societies that's why any information about the provenance of ceramics is highly valuable in the archaeological analysis. In the case of Roman brick-making, the provenance and manufacture of clayey materials are usually interpreted only by studying stamps imprinted on the artefacts, when available. In this paper, the making of bricks, tiles and other ceramics for building purposes is investigated, in relation to the possible sources of raw materials used for the industry. The major questions to be solved relate to the sites from where the Romans collected the raw materials, the technologies they applied to make bricks and other clayey building materials, and how far have they transported raw resources and final products – i.e. mainly bricks and tiles – after furnace treatments, considering that a crucial point was the nearby availability of timber, water, and sandy soils without stones. Some achievements to classify artefacts with identical provenance have been obtained also following the structural transformations induced in the material by thermal treatments of pottery. Comparisons have been made of the chemical composition (ICP-MS analysis) and some physical properties, like magnetic (VSM hysteresis loops) and mineralogical (XRD and IR analysis) features, identified as a proxy to elucidate the possible provenance of rough materials and appreciate the technologies, used by the Roman brick-making industry.

Keywords brick, soil, clay, rare earth elements, magnetism, *Industria*

1. Introduction

Brick represents the man-made ensemble of human artefacts routinely recovered in the archaeological documentation (Skibo and Feinman, 1999; Hodder, 2012). The main constituents are rich-clay soils. The exploitation of bricks and tiles has always been very convenient and useful for humankind, as the raw material is abundant on the earth's surface and easy to shape and fire. Yet, little is known of the making of less refined ceramics, whose enormity of production and trade is surprising in view of the slight knowledge we have of the associated industry. This is the case for bricks and tiles in the Roman age, whose production was one of the most vital manufacturing industries in Roman times with confirmed evidences of export towards the main cities of the Mediterranean (Helen, 1975; Thébert, 2000). Nevertheless, the technological aspects of brick making in ancient Rome, which is thought to have been one of the most important business of the Empire, remain relatively mysterious. Some major questions are related to defining from where the Romans collected the raw materials, how have they made their bricks, and how far have they transported the bricks with respect to the furnaces.

In general, the determination of provenance of archaeological finds is based on two assumptions: i) raw materials from diverse sources have different chemical compositions; ii) variations of composition within one source are smaller than between materials from different sources. In the archaeological context, scientific literature illustrates a wide variety of approaches applied in the study and characterization of soils (Marra, 2011) and ceramics artefacts to gain information on provenance, technology and manufacture, from X-ray diffraction (*e.g.* Rye, 1977) and direct observation of structural phases by scanning electron microscopy, to reflection spectroscopic investigation of the colour of ceramics.

To enlighten the manufacture of bricks and tiles in the Roman territory during the first centuries AD and investigate how the sources of raw materials were selected, we analysed the soil features of an area situated on the left side (North) of the Po river in North Western Italy – in particular, the triangle area comprised between two ancient Roman regions (*Liguria*, *Transpadana*) and one Alpine district (*Alpes Cottiae*) – along with the different chemical and physical properties of soils, bricks, and tiles recovered from Roman sites located in the same region.

Chemical, structural and magnetic analysis were conducted, respectively, using mass spectrometry coupled with inductively coupled plasma (ICP-MS), X-ray diffraction (XRD), infrared spectroscopy (IR), and magnetic measurements.

2. Material and methods

2.1 Spatial and temporal domain – Sampling

Since the Julio-Claudian epoch (0-35 BC) and for census requirements, the Italian territory was divided by Roman government into *Regiones*. So, the actual North-Western Italy corresponded to *Regio IX Liguria*, *Regio XI Transpadana*, and *Alpes Cottiae*, with borders (Figure 1) defined by *Alpes Maritimae* (South-West), *Gallia Narbonensis* (West) and Po river (South).

Accessibility of resources, including the procurement distances for soil as a raw material source, was carefully weighted in ancient societies (Schiffer and Skibo, 1997) and even if in some cases, the distance travelled to reach a clay source has been found to be greater than 50 km, the exploited sources were usually available within a radius of 10 km from the brick-making site (Arnold, 1985). As an ideal raw terrigenous source for bricks does not exist, the soil employed in the brick-making had presumably to fit few criteria: a minimum content in clay (*i.e.* not lower than 20 percent by volume), a practically total lack of soil skeleton, and a small amount of carbonates. Consequently, our selection of the potential sources of raw material for the ancient brick industry started with the scrutiny of soil composition maps related to the investigated area, made available by the Piedmont Region (Regione Piemonte, 2010). We selected soils and building samples from *Regio IX, XI* and *Alpes Cottiae*, in Italy and from *Regio Hispania Baetica* in Spain (samples from Andalusia in the form of fired soils have been largely imported in ancient Italy by Romans. The production of olive oil was transported in amphorae and thousands of their debris are present in Italian settlements).

The straightforward identification of existing material sources in ancient times was not possible, because no open-pit had been discovered in the vicinity of the brick sampling areas. According to our hypothesis, the fluvial terraces most likely exploited in Roman times as clay sources could be identified by comparison of the chemical and physical properties between the chief soil types of the region and the building materials located in the archaeological sites.

In addition, it must be considered that since ancient times, the shorter the distance between the origin of raw materials for building (soil, water and wood for firing) and building sites (kilns and other constructions), the higher is the probability of matching.

In our study (Figure 1), major soil sites have been located in Rovasenda and Vauda at North, Chieri at East, and Cellarengo and Poirino at South-East of former *Augusta Taurinorum* (Torino) and Piscina and Bagnolo along the southern part of the Piedmont plain; soil samples of Andalusia were from Bujalance and Aroche (Table 1). These soil sites have some characters of interest, namely: 1) the content of clay in their upper horizons is less than 25% in Cellarengo and Piscina, around 30-40% in Bene Vagienna, Tortona and Poirino, almost 40% in Rovasenda and Vauda, and greater than 40% in Bagnolo, Bujalance and Aroche (a full description of the pedological features is available at www.regione.piemonte.it); 2) the ratio of sand particles, which is on average 30% of the total volume amount.

All soil data related to B horizons are located at an average depth between 100 and 150 cm. All these soils do not contain stone lines nor rock fragments, and due to their degree of pedogenesis, all of them are sub-acid or acid without carbonates in the upper horizons.

2.2 *Materials*

The rationale of these distributed samplings was to take account of the largest amount of typologies of fired bricks and of the potential sites of raw materials available in the territory. Archaeological samples have been collected from public and private buildings with different uses (kiln, pipeline, wall, …) and constructive typologies (tiles and bricks) (Table 2). In one case, the mark "M·A·[H]", imprinted on the tile from Brandizzo, indicates probably the initials of the *figlina* owner, a local enterprise for the manufacture of bricks (Figure 2).

Furthermore, to verify the reliability of the results, some specimens were selected also from other geographic areas culturally dependent from Rome whose soil fractions were similar to those previously considered, but certainly having a different chemical fingerprint, as in the neighborhoods of the ancient cities *Augusta Bagiennorum* (Bene Vagienna, 44°32'43"N, 7°49'59"E) and *Julia Derthona* (Tortona, 44°53'39"N, 8°51'56"E), in Southern Piedmont (Lomello and Oltrepò soils and Costeggio and Lomello artifacts), and in the former Roman province of Spain, *Hispania Baetica* (geographically located at 37°25′N, 6°01′W) where two soils (Aroche and Bujalance) and three artefacts (Bujalance, Turobriga and Italica) were collected and compared. Finally a NIST 679 "brick clay" certified reference material was used to validate the experimental methodology for chemical analysis.

2.3 Chemical characterization

On the Earth's surface, trace elements are partitioned or separated (enriched or depleted) from each other during geological processes because of differences in their chemical properties. Geochemists use the relative concentrations of trace elements to infer the chemical conditions under which a rock was formed. Specifically, relative enrichments of rare earth elements (REE: La, Ce, Pr, Nd, Sm, Eu, Gd, Tb, Dy, Ho, Er, Tm, Yb, and Lu) are difficult to appreciate as their abundance in soils is scattered. But REE elements always occur together; as a consequence their local differentiation through mobilization and redistribution processes, which can result in fractionation of elements that can therefore be used as tracers of pedogenetic transformations, the latter being extremely long-term processes (Braun et al. 1993; Nesbitt, 1979). For this reason, when investigated, REE patterns may shed some light on past human activity involving soil use (Gliozzo, 2013; Saiano and Scalenghe, 2009). REY (REE plus yttrium) concentrations are usually normalized with respect to different geochemical references; in our case the Upper Continental Crust (UCC) was chosen as reference, which being related to the most accessible part of our planet, has long been the standard for geochemical investigations (Wedepohl, 1995).

To exploit the selective approach in the procedure aimed at inferring provenance through chemical analysis, based on the similarity of the chemical and physical properties of the REE, a feature able to explain their widespread occurrence as a group and their closely common behavior in the environment (Henderson, 1984), ICP-MS instrumental technique was used to investigate the distribution of REY. All chemicals used for the preparation of ICP-MS samples were of ultrapure grade or higher when available and all solutions were prepared with ultrapure water at 18.2 MΩ cm obtained by a Thermo EASYpureII purification system. Working standard solutions for each element were prepared through successive dilution of BDH, Merck or CPI International, 1000 ± 5 μg mL^{-1} elemental standard solution in a HNO_3 1 mol L^{-1} medium. Laboratory equipments were in polyethylene, polypropylene or in Teflon. Determination of trace and minor elements was performed on solutions obtained by microwave digestion of 250 mg of sample with HNO_3, HF, and HCl 3:1:1 (EPA Method 3052). The investigated elements were determined using an Agilent 7500ce ICP-MS spectrometer equipped with a collision cell. Rhodium solution (1ng mL^{-1}) was used as internal standard. Validation of the whole procedure (sample preparation and quantitative measurement) was carried out using certified “light sandy soil” reference material (EU Bureau of

Reference CRM142R/419). Experimental standard deviation, evaluated by replicate analyses, is in the range of ± 10 % for all the investigated elements.

2.4. Mineralogical characterization

X-ray diffraction (XRD) and infrared spectroscopy (IR), were used because of the effectiveness of these techniques to differentiate ceramics samples, as demonstrated in previous studies (Weckler and Lutz 1998; Goffer 2007), focusing on the mineralogical transformation of the clayey matrix upon heating. XRD measurements were performed on powdered fine-earth samples using a Bruker D8 Advance diffractometer (CuKα, 40 KV, 40 mA, antiscatter slit 0.115° 2θ, soller slits 2.5° 2θ) equipped with a LynxEye detector. Sample investigations were recorded in scanning mode and converted to angular patterns (step 0.025°) from 2.5 to 65° (2θ configuration) using 0.6 s or 1.2 s counting time per step. IR measurements were performed on KBr pellets prepared from a mixture of 150 mg of dry KBr and 1.5 mg of dried powder (soil or brick) and analysed on a Nicolet 760 FTIR spectrometer. Spectra displaying the OH-stretching bands (3000-3800 cm^{-1}) were acquired after drying the pellet for one day at 105 °C. In the near infrared region undisturbed samples were analysed using a Nicolet 6700 spectrometer with a wavenumber resolution of 4 cm^{-1} using a NIR DRIFT accessory from SpectraTech.

2.5. Magnetic characterization

In addition to the previously described investigation techniques, magnetisation curves were measured on selected samples to appreciate their magnetic features and follow the evolution of the magnetic properties after thermal treatments. Clay minerals usually contain iron as a minor element, whose total content rarely is above 5 % and is almost entirely converted into pedogenic Fe oxides that give the ferromagnetic properties to the clay matrix. Magnetic measurements are able to evidence the structural changes taking place when clay is heated (La Borgne, 1965; Caitcheon, 1993; Dalan and Banerjee, 1998; Hus et al., 2002; Yang et al., 1993). The oldest literature available for the magnetic properties of ancient ceramics consists of an ensemble of experimental works directed to analyse the technological circumstances under which pottery samples were prepared. The pioneering works were done by Bouchez (1974) and Coey et al. (1979) examining the effects of temperature and reducing atmosphere during thermal treatments on the magnetic properties of iron oxides embedded within ceramics bodies. The determination of firing temperatures was mainly investigated by differential thermal analysis, thermal expansion measurements, and Mossbauer spectrometry, but also magnetic techniques were applied to study the processing of clays and firing conditions of pottery (Coey et al., 1979; Maggetti and Schwab 1982; Tema, 2009). After Van Klinken (2001), who tried to order phase transformations and magnetic properties of iron oxides particles, attention was then mainly focused onto archaeomagnetic dating of ceramics (Fouzai et al., 2012).

For our experiments, the magnetisation curves of tiles and bricks (fragments of mass ~50 mg) were measured on the samples as found, using a Vibrating Sample Magnetometer Vector 7410 Lakeshore (maximum applied field H_M = 1000 mT). Measurements were repeated on different portions of all the samples and the values of the resulting parameters averaged. Since the magnetic behaviour of the samples as found can hardly be attributed directly to the source of the clay-soil used for their production, annealing sequences were applied on selected soil and ceramic samples and the magnetic parameters – such as the coercive field (H_c) and remanence (M_R) – were extracted from the hysteresis cycles and analysed as a function of the applied temperature. This approach has been applied as the subsequent thermal treatments permits to reconstruct the sequence of changing magnetic properties with temperature, which is a specific characteristic of soils still recognizable when the same are turned into artifacts. Thermal treatments were carried out in subsequent 100 °C steps, from room temperature up to 900 °C. Heating was directly applied in the VSM using a thermal-resistance set-up along with a constant field H = 100 mT applied to the sample. Saturation magnetisation (M_S) was calculated after graphic subtraction of the non-ferrimagnetic contributions. Remanence (M_R) corresponds to the magnetisation retained by the sample after the H_M field is released. Comparison of the magnetic properties is made at the end of the annealing sequences; magnetic similarities between samples and clays after thermal treatments can, eventually, be used to appreciate the technological conditions applied for production, such as temperature, atmosphere, and duration of firing (Beatrice et al., 2008).

2.6. Speculation on brick-making technology

In order to provide hypotheses on the provenance of ceramics on the basis of technological and archaeological analogies, experimental replicates of past brick-making technology were used to prepare clay briquettes with volumes about 50 cm^3 (8 x 4 x 1.5 cm; Wolf, 2002). In addition, cubes of approximately 5 cm^3 were dried at 60 °C for one day, and then fired in an electric furnace under oxidising atmosphere at a final temperature of 750 °C for 14 hours (T ramp ~150 °C hr^{-1}). The small cubes were made only of soil mixed with deionised water and showed various hues, from yellow to reddish according to the main colour of the parent soil. As in ancient furnaces, only few cubes immediately adjacent to the chimney conveyor – where temperature is higher – vitrified or cracked while experiencing high temperatures, T >900 °C (Wolf, 2002). Since, in general, the majority of bricks experienced temperatures higher than 600 °C, we estimated for a single kiln load replica experiment an average temperature equal to 750 °C.

In addition, a replica drying experiment was performed with the aim of evaluating the operability of the brick-making process: sesquipedalian bricks (45 x 30 x 10 cm) were formed in wooden boxes without bases, using all the soils sampled matching the ancient *Regio IX*, *XI* and *Alpes Cottiae* (*i.e.* excluding soils sampled for comparison). A variable volume of water has been added to reach the optimal workability of each soil mixture. Then, individual freshly cast bricks were compacted manually and placed on a wooden base insulated from the ground by a sand film, to dry by natural processes for up to three months (Figure 3a).

3. Results

3.1. Provenance of raw material for brick-making

In an attempt to identify any objective parameter differentiating artefacts and soils of different sources as well as any link between artefacts and soil sources, attention was addressed to REY elements. In all samples, in terms of concentrations, cerium, lanthanum, neodymium, and yttrium account for more than 80 % of all the REYs (Table 3) with a nearly symmetrical and platykurtic general distribution (skewness <0.4, kurtosis -1.7/-0.4). A close examination of the REY data allows the identification of some parameters that can be used for discrimination purposes, to find differences or similarities between artefacts and soils, or for provenance assignment of the artefacts themselves. The relationships between the rare earth elements are often used to highlight different behaviours between the light and heavy REE. Therefore, we have calculated the $(\Sigma LREE/\Sigma HREE)_{UCC}$ (*i.e.* the ratio between the content of light REE (from La to Eu) and the content of heavy REE (from Gd to Lu plus Y) and the $(Gd/La)_{UCC}$ molar ratio. In the lower part of Table 3 the values for these parameters are reported for both soils and artefacts.

In particular, considering the $(Gd/La)_{UCC}$ ratio shown in Figure 4, we reported for comparison four different Italian soils and two artifacts of the neighbouring regions (Vagienna, Tortona, Lomello and Oltrepò soils and Costeggio and Lomello artifacts), two Spanish soils (Aroche and Bujalance) and three Spanish artefacts (Bujalance, Turobriga and Italica) and a NIST CRM 679 "brick clay". To obtain information correlating soils with bricks, preliminarily the element abundances in the raw and fired soil samples were compared to verify the conservative role of REYs subjected to the brick-making process. The REY concentrations in the fired samples are on average higher than in the raw ones. The concentration variations appear to be closely related to the mass loss upon firing and the differences in percent loss on ignition are related to the different content of carbonaceous rock and clay minerals. The REY element concentrations reported on a graph for raw *vs* fired soil samples (data not shown) are strongly correlated with a R^2 higher than 0.996. This means that no information on the correlation among the investigated elements is lost during firing and that the raw sample element abundances can be safely used for archaeometric purposes. As can be observed

(Figure 4), soils and artefacts are distributed in groups suggesting the same regional provenance. Along with results in Figure 5 and Table 3, these results suggest a similarity in terms of $\Sigma LREE_{UCC}$, $\Sigma HREE_{UCC}$ and $(Gd/La)_{UCC}$ ratio of the Piedmont soil samples and artefacts as well as a difference with respect to the Spanish samples. The clear but not so trivially predictable differences with soil and artefacts of the neighboring Piedmont regions were interesting too. The large overlapping of soils and artefacts in the $(Gd/La)_{UCC}$ ratio graph did not indicate a direct link between artefacts and potential soil sources. The differences relating to the concentrations of Gd and La, which is higher in artefacts than in soils, are due to the loss of organic substance and carbonates at high temperatures (600-900 °C) when firing is applied to make the artefacts themselves. However, the $\Sigma LREE/\Sigma HREE$ and $(Gd/La)_{UCC}$ ratios do not reveal all the information available on the distribution of the fifteen REY elements studied. For example, since the REY_{UCC} normalized pattern represents a sample fingerprint, its use as a reference to compare similarities or differences of soil and artefact patterns, could support a correlation of the artefacts with their possible soil sources.

In Figure 5a, the REY_{UCC} patterns are shown for all the samples analyzed. In Figure 5b the case of five fragments (V-IX) from *Hasta* is presented: three of them (V, VIII, IX) show a quite complete overlapping of their REY patterns with the soils in their vicinity; this is assumed to be a geochemical proof of the origin of the raw material utilized in their brick-making. Brick VI from the positioning floor of a public building and brick VII from the main sewer conduit under *decumanus* differ slightly. Their patterns show also similarities with REY pattern of tertiary clays *Regio VI Umbria* (Bottaccione near Gubbio 43°21'N 12°34'E, data from Ebihara and Miura, 1996). This fact may open several plausible interpretations, from mixing of the raw material to the long distance transportation of special bricks (*e.g.* for final use or due to their technological characteristic as a sewer conduit). However, these two bricks have not been made using only local soils. The soil of Piscina was the only one of the examination group whose REY_{UCC} pattern did not match any of the considered artefact.

Our results are consistent when superimposed on the map reporting the $(Gd/La)_{UCC}$ ratio distribution in the analyzed region, independently obtained (Figure 6). With this map it is possible to discriminate chemical signatures and individual soil and brick samples of Piedmont from those having other geological and archaeological origins. The $(Gd/La)_{UCC}$ ratio also allows differentiating the inter-site chemical signatures, suggesting possible soil sources for different artefacts.

A thorough analysis of data and REY_{UCC} patterns suggested the relations reported in Table 4. The best artefacts-soils matching available in the explored range was in all cases indicative of local exploitation: the source of raw material matching the REY pattern of bricks is likely to be located within the limits of a one-day terrestrial transport, i.e. an area with a radius between 40 and 70 km. In general, on the basis of a quite large grid of observations, it is possible to guess an intra-*Regio* utilisation of soil as material resource for the local brick industry, except for samples I and II, a tile and a brick respectively, imported from elsewhere. This supposition is supported, in the former case, by the small dimensions of the sample – which favour transportability – and for both cases by their discovery in a clay-poor area.

3.2. Mineralogical characterization

Quartz is the main component of bricks (Figure 3b). It has an angular shape of varying size, from just a few micrometers to several millimeters. This mineral is a natural component of the sediments transported beside the Po River basin, and it is commonly found in similar-sized grains in the soils. This indicates that quartz fragments occurred already in the clay matrix. Technological analogies have been assumed from tempera of the ceramic pieces found in the Roman city of *Basti* (Cultrone et al., 2011). Apart from quartz that prevails in all bricks and tiles, our analysis evidenced the following major components are either plagioclases or K-feldspars. Hornblende, illite, and muscovite-like clay minerals also occur in some samples. Goethite appears in traces in the first two bricks from *Segusio*, while hematite occurs in all samples. Calcite occurs in Andalusian samples only. Mullite does not occur in any sample (Table 5). Soils assumed to be potential sources of raw material for brick-making are always rich in quartz followed by plagioclases, but K-feldspars are not very abundant and often absent. The most common 2:1 phyllosicates are chlorites, muscovite-like and paragonite-like minerals. If chlorite is generally the most abundant of these phases, it is not observed in the three Andalusian soil samples containing carbonates (calcite mainly). Iron oxides as goethite appears in traces in two soils from Vauda and Chieri while hematite does not seem to occur. Soil of Tortona is the only one showing vermiculite and swelling minerals (smectite) as phyllosicate phases.

In general, the possible sources of raw materials match with the qualitative mineralogy of the Roman artefacts. This is well exemplified for a sesquipedalian brick when compared with the soil horizon in which it has been discovered (Figure 7a). However, the mineralogy of crude soils and bricks differs at least partially (Table 5): thermal effects due to firing affect the initial mineralogy and this will be studied in a next section.

3.3. Magnetic characterization

Figure 8 shows the distribution of soils and ceramic fragments according to their magnetic (M_R *vs* H_c) characteristics, as attained by VSM measurements of the magnetization curves at room temperatures. The analysis of magnetization curves is useful for a qualitative evaluation of the magnetic character of the samples. High field slopes of magnetization curves indicate paramagnetic contributions, which can be of paramount importance in ceramic materials fired at low temperatures. Tight loops indicate the presence of a single phase contributing to magnetic coercivity (Atkinson and King, 2005). Samples consisting of multiple magnetic fractions – usually a combination of ferrimagnetic (magnetite, maghemite) and anti-ferromagnetic (hematite, goethite) minerals – show open distorted loops. On the basis of their stable (*i.e.* high M_R, high H_C, large or distorted loops indicating a prevalence of antiferromagnetic particles) or unstable magnetic behaviour (i.e. low M_R, low H_C, linear-reversible loops indicating an important paramagnetic and/or superparamagnetic contribution by smaller iron-oxide particles), samples can be classified into three different groups: 1) magnetically stable ceramics retaining low slope at high fields, tight loops, and high remnant magnetization (only represented by sample VII), 2) less magnetically stable samples, which combine distorted loops with relatively high remnant magnetization (*e.g.* most of the ceramics along with soils 11 and 12), 3) soil samples, plus ceramics VIII and X, exhibiting unstable magnetic properties, characterized by linear-reversible loops, low remnant magnetization, and high slope at high fields.

3.3.1. Variable-temperature magnetic measurements

The magnetic properties of ancient bricks and tiles have been used also to evaluate the technological conditions applied for their production: temperature, atmosphere, and duration of firing (Beatrice et al., 2008). In our case, the magnetic behaviour of the samples evidenced in the as found state can hardly be related to the source of clay-soil used for their production. Therefore, annealing sequences were applied in the temperature range from 400 °C to 900 °C, following the magnetic moment variation (constant applied field H_{max} = 3 kO_e), while the usual magnetic parameters, such as the coercive field (H_c, mT) and remnant magnetization (M_R, Am^2kg^{-1}) were obtained from hysteresis cycles measured after each thermal treatment.

As an example, in Figure 9 the change of magnetic properties with temperature of a tile and clay samples, both collected in Andalusia, within a distance of few kilometres, are reported. In Figure 9a, the magnetic loops measured on the as found samples are compared, showing a similarity already appreciable of the tile XIII with respect to the clay 11 sample. Since magnetic properties vary when thermal treatments are applied at increasing temperature, the correspondence between the two specimens is rather confidently established if the whole plot of the magnetic behaviour with temperature is examined (Figure 9b). Experimental results indicate a close relationship, as evidenced by the common magnetic patterns of the tile (dashed line) and clay (continuous line [red line in colour]) samples in the temperature range from 600 °C to 800 °C. Furthermore, since tile XIII consistently modifies its properties only after experimental heating at 700 °C, it is supposed to have experienced an equivalent temperature treatment in the past between 600 °C and 700 °C. Also, the overlapping of the hysteresis cycles measured on the samples after thermal treatments above 600 °C (Figure 9c) confirms the closeness of the magnetic properties of the soil and artefact. A final comparison is made reporting the thermomagnetic curves of both samples, previously treated at 700 °C, up to 800 °C (Figure 9d): once again similarities are observable in the curve shapes, having two Curie temperature points corresponding, respectively, to titano-magnetite (T_C ~ 550 °C) and titano-hematite (T_C ~700 °C) minerals.

In Figure 10, the same comparison as in Figure 9 is made of the magnetic properties change versus temperature of clay 8 (corresponding to Cellarengo) and ceramic VI (*Hasta*), both located in the South-East area of the investigated region (Figure 1).

Figure 10a shows the large difference in the magnetic loops of the as found soil and ceramic samples. In Figure 10b, it is possible to appreciate that clay 8 enhances its stable ferromagnetic character only after treatment at 600 °C, while the ceramic sample changes its magnetic character after treatment at 700 °C, indicating a value between 600 °C and 700 °C as the equivalent ancient heating temperature also for sample VI. Figure 10c confirms the similarity to sample VI achieved by the magnetic curve of soil 8 after heating at 600 °C; Figure 10d, finally, compares the two similar thermomagnetic curves.

The hysteresis curve of the ceramic IV (Figure 11), found at Brandizzo, suggests an important contribution to the magnetic moment of this sample due to small (paramagnetic and superparamagnetic) iron particles associated with more stable ferrimagnetic grains, probably made of Ti-magnetite. As magnetization increase is linear with the applied field below 300 mT, contributions due to hematite-like minerals are to be excluded. When compared with other ceramic samples, colour and magnetic properties of sample IV suggest that thermal treatment was carried out at temperatures not higher than 750-800 °C.

3.4. Transformation of the soil mineralogy in the consequence of heating

Applying thermal treatments at different temperatures on the reference clays, directly in the thermal chamber of the XRD instrument or in a conventional furnace, we observed significant differences. Several differentiated parameters are able to explain this: e.g. in the XRD thermal chamber the amount of sample is small and the heating kinetics relatively fast, while the sample cannot fill completely the volume of the chamber, as in a conventional furnace. Probably due to these reasons, at any given temperature, the disappearance of primary minerals and the crystallization of secondary phases always attain upper grade in the conventional furnace (Figure 7b); it is possible that the XRD chamber conditions only allow for a metastable state (data not shown). The mineralogy of crude soil 5-Vauda is composed of quartz and plagioclase (albite probably) as major components associated with minor phases as micas, amphibole (hornblende) and K-feldspar (Table 7). After 750 °C heating the 14.1 Å reflection disappears because chlorite is unstable over 600 °C while a reflection appears close to 9.3 Å possibly interpreted as talc or pyrophyllite crystallisation. On the other hand the major peak of plagioclase decreases, which can indicate the beginning of the eutectic transition of this feldspar (Figure 12). The mineralogical composition of soil 8 before thermal treatment is the same as soil 5, except goethite. After heating no 9.3 Å reflecting phase has crystallized and the reflection of the micas (9.7 Å) has disappeared. As for soil 5 at 750 °C the presence of hematite is doubtful because the major peak of this phase is in the same angular position as other phases. The mineralogy of soil 9 after thermal treatment confirms the composition of soil 8 but for a higher content in micaceous phases (10.0 Å). The broad tails of this peak probably indicate a contribution of dehydrated smectite phase.

The mineralogy of brick IV (Brandizzo) is essentially composed of quartz with low contents of feldspar minerals (K-feldspar and plagioclase), with broad peaks (3.24 Å and 3.19 Å respectively) possibly interpreted as a beginning of fusion (over the eutectic point temperature), and traces of amphibole (hornblende probably). Compared with crude clay before the 750 °C thermal treatment the mineralogy of brick IV is without phyllosilicate assemblage (chlorite, mica and probably smectite) that is a difference with all 750 °C soil showing a reflection close to 10.0 Å attributed to mica and dehydrated smectite. Another important difference is the high content in iron oxide (hematite) in brick IV, a mineral whose presence is always doubtful in experimentally heated soil samples (Figure 12) as the kinetics of heating process is generally too fast to obtain a well crystallized phase.

The FTIR analysis provides additional information, complementary to XRD analysis. In the 1100–400 cm^{-1} region, bands corresponding to Si–O and Si–O–Si, and Al–O and Al–O–Al were detected in all of the archaeological samples. These vibrational bands could be attributed to the muscovite, feldspars, and quartz. Appearance of bands at 1096 cm^{-1} and 630 cm^{-1} could be used as FTIR reflectance spectra indicators of previous heating treatment in the temperature range 400-550 °C (Berna et al., 2012). On the contrary, the mid-IR spectra of the soil and of the soil samples heated up to 950 °C are similar. The mid-IR spectra of the soil 5 samples heated at 680 and 950 °C are very similar to the bricks II and VI spectra. The only difference comes from calcite (bands at about 1450, 875, …) whose occurrence is evidenced in the bricks, but not in the heated samples. This is in accordance with the XRD data (Table 5). The near-IR spectra of the soil heated at 680 °C is similar to the brick II and VI (Fig 13). The NIR spectra of the soil 5 samples heated at 680 and 950 °C are very similar as well to the bricks XI spectra. The only difference is the kaolinite disappearance for the heated samples; disappearance of the bands due to kaolinite at about 3700 and 3620 cm^{-1} (Figure 14a). The spectrum of the sample heated at 1100 °C clearly differs. It reveals broad bands due to vitrification of the minerals (Figure 14a and 14b). These analogies confirm the matching between Roman bricks and most probable soils utilised as raw material based on the REY_{UCC} pattern (Table 3).

4. Discussion

The samples examined show a close correlation between the point of use and discovery and soils from which they originated. Moreover, the lack of additives in the mixtures shows that the production of bricks was little influenced by the location of the resource "clay", but much more by that of water and, above all, fuel for the furnaces. Woodland areas were not generally part of the lands granted to settlers as commons use by the community for cutting wood (*silva publica*) (Settis et al. 1984).

The assumption, therefore, must be that bricks were produced in a short distance from places of employment and exceptional cases (other known brands in other areas, no structures in the locality where the predominant soil types is found, or prevailing use of stone in the buildings) must be analyzed on the basis of historical data available for the individual sites. In the Roman Empire, forest clearance occurred fundamentally for obtaining arable land but also retrieving wood for other uses and as a consequence, the Mediterranean underwent intensive deforestation (Certini and Scalenghe, 2011; Wertime, 1983; Williams, 2000). During Roman times in northern Italy, more than one third of the mountain forest cover disappeared and two thirds of the floodplain was cleared (Cremaschi et al., 1994; Cremonini et al., 2013; Drescher-Schneider, 1994). Nevertheless, the extent of deforestation (Farabegoli et al., 2004; Kaplan et al.; 2009; Zanchetta et al., 2013), although not influenced primarily by the brick-making industry, was, probably, a consequence of it.

4.1. Brick-making technology

Sun-baked and unfired brick use dated from the beginning of the Holocene in the Middle East. The technology of firing bricks arrived probably centuries later from Mesopotamia to Europe and China, where sections of the Great Wall were partly built with burned bricks, and through the Middle East it reached Persia and India. In Europe, the Romans emulated their first expertise in building from the Etruscans, although Greek influence was maintained in sizing. Being cheaper than stone-working, brick-making became during Roman times one of the most important industries and a state monopoly under the Empire. The Romans refined the Etruscan brick-making technology in the selection and preparation of the raw material and in the design of the kilns.

The soil material in modern brickmaking, once extracted, is left ventilating indoor for a few months (maturation). The purpose is to regulate the humidity of the material before firing, to avoid fractures. There is no an analytical to confirm that the 'maturation' of the soil dug before cooking a modern brick occurred also in Roman age. Nor it is possible to determine analytically on a two thousand years old sesquipedalian brick that this practice was certainly adopted but it is likely that a ‘fermentation’ or ‘maturation’ was already in use at the time of the Romans.

After grinding, tempering, moulding, drying, and dressing, bricks were fired until the requisite hardness was obtained conferring them a resistance to weathering comparable to those of stones, which were much more difficult to work.

The terrigenous materials must be mixed with water to form the finished product, and the amount of added water depends on the nature and plasticity of the soils in addition to the dominated temperature and air currents. The bricks, after being manufactured, must be dried as they could burst out if heated without drying. Today bricks are manufactured by mixing soils with water to attain plastic mechanical properties, then squeezing them with pressures as high as thousands kPa in rectangular steel columns, finally cutting the individual units. Romans formed bricks using more water than today and placing the plastic mixture in wooden molds lubricated with sand or water. There is evidence that the raw soil material would have not required any addition but homogenisation only (Benea et al., 2010; Eramo and Maggetti, 2013).

Actually, bricks are normally fired in a continuous oven-type chamber. The maximum temperature practically attainable is 1100 °C after one week of burning. Romans used heated enclosures as up-draught periodic kilns that, although being designed essentially on insulation, obtained a poor internal temperature distribution and hence an irregular firing of the bricks inside. The bottom part of the kiln adjacent to the firebox experienced higher internal temperature (T ~1100 °C); heating conditions reduced gradually as naturally occurring convection fluxes conveyed heat towards the top of the kiln, approximately at a temperature lower than 800 °C, equivalent to the highest temperature of a small bonfire. Within the kiln, only 10% of bricks experienced temperatures higher than 950 °C or lower than 650 °C (Wolf, 2002). The principal determinant of the capacity of a brick factory is – and probably was – the size and number of kilns; in ancient time, it was also the availability of wood. Brick plants built during the 1960s had a production capacity of approximately 20 million extruded bricks per year; a modern brick plant can produce 100 million bricks per year (Scheibl and Wood, 2005). Kiln functioning is today the bottleneck of brick production, and probably it was the same in ancient times.

The internal volume of Roman kilns probably ranged between 5 and 40 m^3 (Darvill and McWhirr, 1984; Jackson et al., 1973). The few Roman kilns for bricks discovered in Piedmont have cooking chambers approximately measuring 11-14 m^2, their height is unknown. It was calculated for a chamber of 9 m^2, a batch capacity of 3,500 tiles (Barberan et al., 2002).The kilns burnt thousands of cubic meters of wood, at a rate as high as hundreds of cubic meters per year.

Estimating the manpower required in ancient time to form a brick is quite difficult. The labour force constraints in the brick-making industry pose different questions. The time required during Roman times for digging (including the unknown average depth), processing and firing have been only conjectured. For this reason, we shaped sesquipedalian bricks (45 x 30 x 10 cm) in wooden boxes in order to provide hypotheses on the labour requirement for brick production. In our replica experiment (Figure 3a) independently on the type of soil, full processing (excluding digging and firing) takes one unskilled man-day for ten *sesquipedales*, roughly 1,000 *sesquipedales* for 1 skilled man-month applying a unskilled/skilled coefficient of 0.4 (Delaine, 2001).

4.2. Structural transformations during the firing of bricks

The soils of the study area contain quartz, plagioclase, chlorite, muscovite-like and paragonite-like minerals, some of them contain K-feldspath, smectite, illite, hornblende, and goethite (Table 5). The only differences in comparison with Roman bricks are the lack of paragonite-like minerals and the sparse appearance of gehlenite and pyroxene (Table 5). Most of the changing in mineralogy occurs between 680 and 750 °C (Table 6, Figure 10b). In fact, when the assemblage of aluminium silicates, iron oxides, organic carbon and carbonates, and other more soluble salts of a soil is fired at an appropriate temperature, irreversible chemical changes take place (Wolf, 2002). The final product turns, in general, into a durable material through transformations that develop with temperature (Table 7):

- heating to moderate temperatures below 300 °C enhances the magnetic fabric in bricks (Hus et al., 2002), then
- maghemite may form at temperatures >300 °C (e.g. when “green” wood is used for firing, because of the reducing atmosphere created by the smoke emitted by this fuel; Setti et al., 2006), but
- below 400 °C, if the soil material is oxidized, porosity increases (if the heating takes place under reducing conditions, the remaining carbon turns into dark charcoal filling the pores),
- between 400 and 650 °C, dehydration takes place, OH-groups are removed from the structure of silicates and these hydroxyls are lost into the atmosphere, irreversibly altering clays and metal oxides (in ancient times, bricks were fired to temperatures commonly above 600 °C),
- above 700 °C clayey material is considered definitely fired, in fact a well-fired pottery turns virtually inert and durable, assuming a reddish colour, confirmed by the presence of haematite,
- kaolinite may turn thermally into a ‘slightly disordered’ metakaolin just above 800 °C (Murad and Wagner, 1991) when all carbonates eventually present are lost and iron oxides turn entirely red and become a very stable material with a porosity higher than 20%, but increasing the vitrification process porosity diminishes,
- spinel structures can form over 900 °C (bricks are then blackened or greyed if the atmosphere in the kiln is converted into reducing conditions, mainly thanks to organic matter conversion into unburned carbon particles), then
- at temperatures higher than 900 °C the incipient vitrification reduces the porosity (which at 1100 °C reduces to less than 5 %); large earthenware vessels were fired at such high temperatures for purposes of sealing them,
- illite/muscovite disappear completely above 950 °C (Benea et al., 2010; Cultrone et al., 2011) while, depending on the initial composition of the raw material, mullite, gehlenite, and diopside

begin to appear (when temperatures exceed 900 °C the presence of calcite enhances the stability of newly-formed gehlenite, which may persist up to 1075 °C, after that even the degree of anisotropy of magnetic susceptibility decreases; Hus et al., 2002; Maniatis et al. 1981, 1983; Setti et al., 2006),

— at 1200–1300 °C, the highest temperature attainable in most ancient kilns, a very strong and translucent ceramic material occurs, stoneware, with a total porosity <2%, above these temperatures,

— total melting is expected (temperatures improbable to be attained by men in antiquity; Goffer, 2007; Pollard and Heron, 2008).

5. Conclusions

A synopsis of the three main questions addressed by this manuscript (1, from where the Romans collected the raw materials?; 2, how have they made their bricks?; 3 how far have they transported the bricks with respect to the furnaces?) could be that in Roman brick-making soil characteristics were not essential, as they transported raw soil material usually for distances of only a few kilometres. Key points in order of importance were availability of timber and water and soils without stones.

The Romans, after having clear-cut an area, used some soil horizons suitable for their direct transformation into fired and unfired bricks. These soil horizons in the foothills of the Alps were also certainly horizons of impediment to the growth of plants (*e.g.* argillic, fragipan). Since the 'brick' quarries presumably could not be very deep, after their logging and the removal of some soil horizons, the Romans established agriculture that, was not in antagonism but in synergy with the brick industry. Archaeologists have not yet reported finding quarries of Roman age devoted entirely to the brick industry. Probably this results from the subsequent transformation of the landscape, as the forest-agriculture shift remains more evident than small topographic anthropogenic remodelling, traces of which have been lost over two millennia.

The sesquipedalian brick has been culturally inherited from the Greeks who had develped bricks of this volume to build big, sometimes very huge items. As no calculations were made in the structural design of buildings, their over-sizing was necessary and was easily obtained with sesquipedalian. In addition to aesthetic and cultural reasons, there are geometric reasons and standardization constraints imposing the uncomfortable (from a technological point of view) size of Roman brick. The type of soil did not affect the production technology of Roman bricks, which differs (very slightly) geographically only for cultural reasons.

Our idea explained in this work was to evaluate the predominately analytical techniques to verify the specific utility and their effectiveness in the specific case of bricks and tiles, summarising our findings compared to the current literature (Table 8). Bricks are ubiquitous materials and 'trivial' from an archaeological point of view. Rare are the stamped bricks or tiles. For this reason, the only keys of archaeological investigation are not sufficient to clarify the suppositions about the originating materials used in the brick-making industry. This happens even when laboratory routine methods are coupled. The mineralogy of bricks, their content of major chemical elements, or their magnetic behaviour provides no information explaining the origin of raw material used.

In particular, only rare earth elements plus yttrium (REY) provide keys useful to help us understand the geographical origin of the materials used in the manufacture of bricks or tiles, even in the absence of archaeological evidence (*e.g.* furnaces) and ICP-MS appears to be an ideal method to study archaeological samples because of its good detection limits, precisions, accuracies and multi-elemental determination. Clues on technology in the brick-making can only be reached by the combined use of different techniques: either more traditional ones, such as optical microscopy and diffraction, or the more recent ones. In particular, magnetic techniques allow establishing with precision the maximum temperature to which the material has been subjected. Therefore, the possibility to discriminate the provenance regions opens new perspectives in the studies of archaeological bricks, to understand the trade routes at different periods. Nevertheless, it will necessitate in the future important work to characterize the typical signature of each region of interest.

Acknowledgments

Région Poitou-Charentes kindly supported first author. DISAFA-Università di Torino has made available its laboratories for some of the analyses. ARPA Piemonte has provided data on the Gd/La ratio. Hamish Forbes and Giuseppina Spagnolo Garzoli provided extremely useful and valuable information. The Carena family from Cambiano kindly has made available its historical experience in the manufacture of bricks. Carlos Odriozola and Antonio Delgado from the Universidad de Sevilla friendly provided the Andalusians samples. We are further indebted as well to Rosanna Nardi for providing Figure 2b. We wish to express extreme gratitude to Peter Randerson from Cardiff University for the time he generously devoted to reading and reviewing this manuscript.

References

Alonso, E., Sherman, A.M., Wallington, T.J., Everson, M.P., Field, F.R., Roth, R., Kirchain, R.E., 2012. Evaluating rare earth element availability: a case with revolutionary demand from clean technologies. Environmental Science & Technology 46, 3406–3414.

Arnold, D.E., 1985. Ceramic Theory and Cultural Process. Cambridge University Press, Cambridge.

Atkinson, D., King, J.A., 2005. Fine particle magnetic mineralogy of archaeological ceramics. Journal of Physics: Conference Series 17, 145–149.

Barberan, S., Maufras, O., Petitot, H., Pomarèdes, H., Sauvage, L., Thernot, R., 2002. Les *villae* de La Ramière à Roquemaure, Gard. Monographies d'Archéologie Méditerranéen 10, 889–919 [in French].

Barello, F., 2004. Brandizzo – Un Insediamento Rurale di Età Romana. Edizioni Relazioni Esterne TAV, Roma [in Italian].

Beatrice, C., Coïsson, M., Ferrara, E., Olivetti, E.S., 2008. Relevance of magnetic properties for the characterisation of burnt clays and archaeological tiles. Physics and Chemistry of the Earth 33, 458–464.

Benea, M., Gorea, M., Har, N., 2010. Tegular materials from Sarmizegetusa – 2. Mineralogical and physical characteristics of the raw material. Romanian Journal of Materials 40, 228–236.

Berna, F., Goldberg, P., Horwitz, L.K., Brink, J., Holt, S., Bamford, M., Chazan, M., 2012. Microstratigraphic evidence of in situ fire in the Acheulean strata of Wonderwerk Cave, Northern Cape province, South Africa. Proceedings of the National Academy of Sciences 109, E1215–E1220.

Bouchez, R., Coey, J., Coussement, R., Schmidt, K., Van Rossum, M., Aprahamian, J., Deshayes, J., 1974. Mössbauer study of firing conditions used in the manufacture of the grey and red ware of Tureng-Tepe. Journal of Physique 35, 541–546.

Braun, J.J., Pagel, M., Herbillon, A., Rosin, C., 1993 Mobilization and redistribution of REEs and thorium in a syenitic lateritic profile – A mass-balance study. Geochimica et Cosmochimica Acta 57, 4419–4434.

Caitcheon, G.G., 1993. Applying environmental magnetism to sediment tracing. In: Peters, N., Hoehn, E., Leibundgut, C., Tase, N., Walling, D. (Eds.) Tracers in Hydrology. International Association of Hydrological Sciences, Wallingford, pp. 285–292.

Calliari, I., Canal, E., Cavazzoni, L., Lazzarini, S., 2001. Roman bricks from the Lagoon of Venice: a chemical characterization with methods of multivariate analysis. Journal of Cultural Heritage 2, 23–29.

Certini, G., Scalenghe, R., 2011. Anthropogenic soils are the golden spikes for the Anthropocene. The Holocene 21, 1269–1274.

Coarelli, F., 2000. L’inizio dell’*opus testaceum* a Roma e nell’Italia romana. In: Boucheron, P., Broise, H., Thébert, Y., (Eds.) La Brique Antique et Médiévale. Production et Commercialisation d’un Materiau. École Française, Roma, pp. 87–95 [in Italian].

Coey, J., Bouchez, R., Dang, N.V., 1979. Ancient techniques. Journal of Applied Physics 50, 7772–7777.

Cremaschi, M., Marchetti, M., Ravazzi, C., 1994. Geomorphological evidence for land cleared from forest in the central Po plain (Northern Italy) during the Roman period. In: B. Frenzel. (Ed.) Evaluation of Land Surfaces Cleared from Forest in the Mediterranean Region During the Time of the Roman Empire. Gustav Fischer Verlag, Stuggart, pp. 119–132.

Cremonini, S., Labate, D., Curina, R., 2013. The late-antiquity environmental crisis in Emilia region (Po river plain, Northern Italy): Geoarchaeological evidence and paleoclimatic considerations. Quaternary International doi:10.1016/j.quaint.2013.09.014

Cultrone, G., Molina, E., Grifa, C., Sebastián, E., 2011. Iberian ceramic production from Basti (Baza, Spain): first geochemical, mineralogical and textural characterization. Archaeometry 53, 340–363.

Dalan, R.A., Banerjee, S.K., 1998. Solving archaeological problems using techniques of soil magnetism. Geoarchaeology 13, 3–36.

Darvill, T., McWhirr, A., 1984. Brick and tile production in Roman Britain: models of economic organisation. World Archaeology 15, 239–261.

De Boer, C.B., Dekkers, M.J., 2001. Unusual thermomagnetic behaviour of haematites: neoformation of a highly magnetic spinel phase on heating in air. Geophysical Journal International 144, 481–494.

Delaine, J., 2001. Exploring the economics of building techniques at Rome and Ostia. In: Mattingly, D.J., Salmon, J. (Eds) Economies Beyond Agriculture in the Classical World. Routledge, Abingdon, pp. 230–268.

Drescher-Schneider, R., 1994. Forest, forest clearance and open land during the time of the Roman empire, in northern Italy (the botanical record). In: B. Frenzel (Ed.) Evaluation of Land Surfaces Cleared from Forest in the Mediterranean Region During the Time of the Roman Empire. Gustav Fischer Verlag, Stuggart, pp. 23–58.

Ducati, P., 1927. Storia dell'Arte Etrusca. Rinascimento del Libro, Firenze [in Italian].

Dunlop, D.J., Ozdemir, O., 1997. *Rock Magnetism. Fundamentals and Frontiers*. Cambridge University Press, Cambridge.

Ebihara, M., Miura, T., 1996. Chemical characteristics of the Cretaceous-Tertiary boundary layer at Gubbio, Italy. Geochimica et Cosmochimica Acta 60, 5133–5144.

Echajia, M., Kacim, S., Hajjaji, M., 2006. Structural change and firing characteristics of a dolomitic clay. Annales de Chimie-Science des Materiaux 31, 23–30.

Eramo, G., Maggetti, M., 2013. Pottery kiln and drying oven from *Aventicum* (2nd century AD, Ct. Vaud, Switzerland): raw materials and temperature distribution. Applied Clay Science 82, 16–23.

Facchinelli, A., Sacchi, E., Mallen, L., 2001. Multivariate statistical and GIS-based approach to identify heavy metal sources in soils. Environmental Pollution 114, 313–324.

Farabegoli, E., Onorevoli, G., Bacchiocchi, C., 2004. Numerical simulation of Holocene depositional wedge in the southern Po Plain-northern Adriatic Sea (Italy). Quaternary International 120, 119–132.

Fouzai, B., Casas, L., Ouazaa, N.L., Álvarez, A., 2012. Archaeomagnetic data from four Roman sites in Tunisia. Journal of Archaeological Science 39, 1871–1882.

Gendler, T.S., Shcherbakov, V.P., Dekkers, M.J., Gapeev, A.K., Gribov, S.K., McClelland, E., 2005. The lepidocrocite-maghemite-haematite reaction chain–I. Acquisition of chemical remanent magnetization by maghemite, its magnetic properties and thermal stability. Geophysical Journal International 160, 815–832.

Gliozzo, E., 2013. Stamped bricks from the *ager cosanus* (Orbetello, Grosseto): integrating archaeometry, archaeology, epigraphy and prosopography. Journal of Archaeological Science 40, 1042–1058.

Hatcher, H., Kaczmarczyk, A., Scherer, A., Symonds, R.P., 1994. Chemical classification and provenance of some Roman glazed ceramics. American Journal of Archaeology 98, 431–456.

Helen, T., 1975. Organization of Roman Brick Production in the First and Second Centuries AD: An Interpretation of Roman Brick Stamps. Suomalainen Tiedeakatemia, Helsinki.

Henderson, P., 1984. Rare Earth Element Geochemistry. Elsevier, Amsterdam, pp. 1–29.

Hodder, I., 2012. Entangled. Wiley-Blackwell, Chicester.

Hus, J., Ech-Chakrouni, S., Jordanova, D., 2002. Origin of magnetic fabric in bricks: its implications in archaeomagnetism. Physics and Chemistry of the Earth 27, 1319–1331.

Jackson, D.A., Biek, L., Dix, B.F., 1973. A Roman lime kiln at Weekley, Northants. Britannia 4, 28–140.

Kaplan, J.O., Krumhardt, K.M., Zimmermann, N., 2009. The prehistoric and preindustrial deforestation of Europe. Quaternary Science Reviews 28, 3016–3034.

Khalfaoui, A., Hajjaji, M., 2009. A chloritic-illitic clay from Morocco: temperature-time-transformation and neoformation. Applied Clay Science 45, 3–89.

La Borgne, E., 1965. Les proprietes magnetiques du sol. Application a la prospection des sites archaeologiques. Archaeo-Phyika 1, 1–20 [in French].

López, F.A., Ramirez, M.C., Pons, J.A., López-Delgado, A., Alguacil, F.J., 2008 Kinetic study of the thermal decomposition of low-grade nickeliferous laterite ores. Journal of Thermal Analysis and Calorimetry 94, 517–522.

Lopez-Arce, P., Garcia-Guinea, J., 2005. Weathering traces in ancient bricks from historic buildings. Building and Environment 40, 929–941.

López-Arce, P., García Guine, J., Gracia, M., Obis, J., 2003. Bricks in historical buildings of Toledo City: characterisation and restoration. Materials Characterization 50, 59–68.

Maggetti, M., Schwab, H., 1982. Iron age fine pottery from Chatillon-s-Glane and the Heuneburg. Archaeometry 24, 21–36.

Maniatis, Y., Simopoulos, A., Kostikas, A., 1981. Mössbauer study of the effect of calcium content on iron oxide transformations in fired clays. Journal of the American Ceramic Society 64, 263–269.

Maniatis, Y., Simopoulos, A., Kostikas, A., Perdikatsis, V., 1983. Effect of reducing atmosphere on minerals and iron oxides developed in fired clays: the role of Ca. Journal of the American Ceramic Society 66, 773–781.

Marengo, E., Aceto, M., Robotti, E., Liparota, M.C., Bobba, M., Pantò, G., 2005. Archaeometric characterisation of ancient pottery belonging to the archaeological site of Novalesa Abbey (Piedmont, Italy) by ICP–MS and spectroscopic techniques coupled to multivariate statistical tools. Analytica Chimica Acta 537, 359–375

Marra, F., Deocampo, D., Jackson, D., Ventura, G., 2001. The Alban Hills and Monti Sabatini volcanic products used in ancient Roman masonry (Italy): an integrated stratigraphic, archaeological, environmental and geochemical approach. Earth-Science Reviews 108, 115–136.

Meloni, S., Oddone, M., Genova, N., Cairo, A., 2000. The production of ceramic material in Roman Pavia: an archeometric NAA investigation of clay sources and archaelogical artifacts. Journal of Radioanalytical and Nuclear Chemistry 244, 553–558.

Mirti, P., Zelano, V., Aruga, R., Ferrara, E., Appolonia, L., 1990. Roman pottery from *Augusta Praetoria*: a provenance study. Archaeometry 32, 163–175.

Morris, A.H., 1994. Canted Antiferromagnetism: Hematite. World Scientific Publishing Company, London.

Murad, E., Wagner, U., 1991. Mössbauer spectra of kaolinite, halloysite and the firing products of kaolinite: new results and a reappraisal of published work. Neues Jahrbuch für Mineralogie 162, 281–309.

Nardi, R., 2011. I laterizi bollati da Industria. In: Zanda, E. (Ed.) Industria. Città Romana Sacra a Iside. Umberto Allemandi & C, Torino, pp. 143–145 [in Italian].

Nesbitt, H.W., 1979. Mobility and fractionation of rare earth elements during weathering of a granodiorite. Nature 279, 206–210.

Pollard, A.M., Heron, C., 2008. Archaeological Chemistry, 2nd edition. The Royal Society of Chemistry, Cambridge.

Rathossi, C., Pontikes, Y., 2010. Effect of firing temperature and atmosphere on ceramics made of NW Peloponnese clay sediments. Part I: reaction path, crystalline phases, microstructure and colour. Journal of the European Ceramic Society 30, 1841–1851.

Regione Piemonte, 2010. Carta dei Suoli del Piemonte 1:250.000 [in Italian]. WebGIS at URL www.regione.piemonte.it/agri/suoli_terreni/suoli1_250/carta_suoli/gedeone.do

Rice, P.M., 1987. Pottery Analysis: a Source Book. University of Chicago Press, Chicago.

Rye, O.S., 1981. Pottery Technology: Principles and Reconstruction. Taraxacum, Washington DC.

Saiano, F., Scalenghe, R., 2009. An anthropic soil transformation fingerprinted by REY patterns. Journal of Archaeological Science 36, 2502–2506.

Scheibl, F., Wood, A., 2005. Investment sequencing in the brick industry: an application of grounded theory. Cambridge Journal of Economy 29, 223–247.

Schiffer, M.B., Skibo, J.M., 1997. The explanation of artifact variability. American Antiquity 62, 27–50.

Schwertmann, U., Cornell, R.M., 2000. Iron Oxides in the Laboratory: Preparation and Characterization. Wiley-VCH, Weinheim.

Setti, M., Nicola, C., López-Galindo, A., Lodola, S., Maccabruni, C., Veniale, F., 2006. Archaeometric study of bricks from the ancient defence walls around the town of Pavia in northern Italy. Materiales de Construcción 56, 5–23.

Settis, S., 1984. Misurare la Terra: Centuriazione e Coloni nel Mondo Romano. Edizioni Panini, Modena [in Italian].

Skibo, J.M., Feinman, G.M., 1999. Pottery & People. Foundations of Archaeological Inquiry. University of Utah Press, Chicago.

Soil Survey Staff, 1999. Soil Taxonomy: A Basic System of Soil Classification for Making and Interpreting Soil Surveys, 2nd edition Handbook 436. Natural Resources Conservation Service of the United States Department of Agriculture, Washington DC.

Tema, E., 2009. Estimate of the magnetic anisotropy effect on the archaeomagnetic inclination of ancient bricks. Physics of the Earth and Planetary Interiors 176, 213–223.

Thébert, Y., 2000. Transport à grande distance et magasinage de briques dans l'Empire Romain. In: Boucheron, P., Broise, H., Thébert, Y. (Eds.) La Brique Antique et Médiévale. Production et Commercialisation d'un Matériau. École Française, Roma, pp. 342–356.

Van Klinken, J., 2001. Magnetization of ancient ceramics. Archaeometry 43, 49–57.

Velde, B., Druc, I.C., 1999. Archaeological Ceramic Materials: Origin and Utilization. Springer, Berlin.

Weckler, B., Lutz, H.D., 1998. Lattice vibration spectra. Part XCV. Infrared spectroscopic studies on the iron oxide hydroxides goethite (α), akaganéite (β), lepidocrocite (γ), and feroxyhite (δ). European Journal of Solid State and Inorganic Chemistry 35, 531–544.

Wedepohl, H., 1995. The composition of the continental crust. Geochimica et Cosmochimica Acta 59, 1217–1239.

Wertime, T.A., 1983. The Furnace versus the Goat: The pyrotechnologic industries and Mediterranean deforestation. Journal of Field Archaeology 10, 445–452.

Williams, M., 2000. Dark ages and dark areas: Global deforestation in the deep past. Journal of Historical Geography 26, 28–46.

Wolf, S., 2002. Estimation of the production parameters of very large medieval bricks from St. Urban, Switzerland. Archaeometry 44, 37–65.

Woods, W.I., 2003. Development of Anthrosol research. In: Lehmann, J. *et al*. (Eds.) Amazonian Dark Earths: Origin, Properties, Management. Kluwer Academic Publishers, Dordrecht, pp. 3–14.

Yang, S., Shaw, J., Rolph T., 1993. Archaeointensity studies of Peruvian pottery from 1200 BC to 1800 AD. Journal of Geomagnetism and Geoelectricity 45, 1193–1207.

Zanda, E., 2007. Tra Industria e Vardacate. L'Insediamento di Mombello e le Presenze di Età Romana in Valcerrina. Museo Civico, Casale Monferrato [in Italian].

Zanchetta, G., Bini, M., Cremaschi, M., Magny, M., Sadori, L., 2013. The transition from natural to anthropogenic-dominated environmental change in Italy and the surrounding regions since the Neolithic: An introduction. Quaternary International 303, 1–9.

Zanda, E., 2011. Industria – Città Romana Sacra a Iside. Umberto Allemandi & C, Torino [in Italian].

Zdujic, M., Jovalekic, C., Karanovic, L., Mitric, M., Poleti, D., Skala, D., 1998. Mechanochemical treatment of α-Fe_2O_3 powder in air atmosphere. Materials Science Engineering A245, 109–117.

CAPTION TO FIGURES

Figure 1. North-Western Italian territories controlled by Romans during Augustus times and locations of sites described in this paper (archaeological samples, filled crosses and soil samples, filled stars). *Regio IX* and *XI* were separated by the river *Eridanus*, Po in grey color. The province of Cottian Alps (bold line roughly parallel to the 7th meridian) secured the communications over the Alpine passes, its capital was *Segusium*, in our days Susa. The cities of *Lemencum*, Chambéry, *Augusta Praetoria*, Aosta, *Eporedia*, Ivrea, *Vercellae*, Vercelli, *Novaria*, Novara, *Mediolanum*, Milan, *Augusta Taurinorum*, Turin, *Brigantium*, Briançon, *Forum Vibii Caburrum*, Cavour, *Carreum Potentia*, Chieri, Vardacate, Casale Monferrato, *Hasta*, Asti, *Pollentia*, Pollenzo, *Forum Fulvii*, near to Alessandria, *Dertona*, Tortona, *Aquae Statiellae*, Acqui Terme, *Alba Pompeia*, Alba, *Augusta Bagiennorum*, close to Bene Vagienna that exists today. *Industria*, formerly *Bodincomagus*, was abandoned during the V century. Regional (— • —) and municipal (— • • —) borders, centuriations (······) and/or their orientations, and main roads, when known, are indicated as lines. [Adapted from de Guillaume de Lisle (1715) *Tabula Italiae Antiquae in Regiones XI ab Augusto divisae* and Zanda (2007, 2011)]

Figure 2. a) Brandizzo (45°10'36.11''N 7°49' 8.43''E, former *Regio Transpadana*), right bank of the river Bendola, Italy. Tiles and walls fall of a roman country house, *villa rustica* (archaeological tiles III and IV, ✚ in Figure 1), consisting of a main building (54 by 60 meters), two large courtyards, *cohortes*, around which there are stockrooms for foodstuff, small rooms of the residence of the tenants, gardens and fences for husbandry, *maceriae*. A few dozen of meters West from the main building a small square (side 12.5 meters) could be seen as a dryer for cereals, *fumarium*. The *villa* is positioned approximately in the middle of one of the four parts into which it is theoretically divisible a century, *centuria*, a hundred *heredia* or two hundred *jugera*, the common measure of land among the Romans (Barello, 2004), b) The stamp M•A•H is attributable to the owner of *figlina*

(brickmaking local enterprise) or its conductor, in charge of management. M•A•H are probably the *tria nomina* initials, the Roman naming system, where M is the *praenomen* (given name of *Marcus*), A is the *nomen gentilicium* (family name: the possible name of the *gens* is virtually countless), H the *cognomen* (distinctive personal nickname, with many different alternatives). This stamp is presently known in the towns of *Industria* and *Augusta Taurinorum*, and in its surroundings, Settimo Torinese, Brandizzo (Nardi, 2011), c) M•A•H stamp on a tile incorporated within the NW wall of the main church in Monteu da Po (former *Industria*).

Figure 3. a) Replica brickmaking of sesquipedalian bricks (45 x 30 x 10 cm) were formed in a) wooden boxes without bases, b) using all the soils, c) individual freshly cast brick was placed on a wood basis insulated from the ground by a sand film, d) to dry for duration up to three months. **b)** Optical microscopy micrographs of seven bricks sampled in the site XI-*Industria* (45°09’32.98”N 8°01’08.25”E, 170 m a.s.l.) [samples have been sawed in dried conditions, one face was successively polished on abrasive disks of 10, 5 and 1 µm size-grain].

Figure 4. Gadolinium *vs.* lanthanum (µmol kg^{-1}). Diamonds indicate bricks while squares indicate soils. In italics data from Meloni et al. (2000). Filled symbols refer to andalusian materials and soils from the former Imperial Roman province *Hispania Baetica* while circle is a reference “brick clay” material.

Figure 5. a) REY_{UCC} pattern for all samples analyzed. Normalized diagram arranged following the periodic table by group. In ordinates REY_{sample}/REY_{UCC}. Diamonds and dotted lines indicate bricks while squares and solid lines indicate soils. **b)** REY_{UCC} pattern for all samples from Hasta and soils (1, 6 and 8) in the neighborhood of 50 kilometers. Archaeological samples VI and VII, are in grey while filled symbols indicate the medians ±SD of REY of tertiary clays *Regio VI Umbria* (Bottaccione near Gubbio 43°21'N 12°34'E).

Figure 6. ($(Gd/La)_{UCC}$ ratio. Thin crosses indicate a measured Gd/La ratio in Roman bricks while bulky crosses indicate the same ratio in soils. Dotted lines are iso-ratio lines of independent measures (ARPA Piemonte data) from A, B and C soil horizons [aqua regia extracts analysed with Agilent 7500ce ICP-MS, contour maps from ordinary Kriging, linear model, nugget 0.02, direction -55; N=534].

Figure 7. a) Comparison of X-ray powder diffraction patterns of Poirino soil (1) and a sesquipedalian brick from Cava Carena in Poirino (1*). The mineral phases identified are: chlorite (Ch), mixed-layer (ML), illite or mica 1 (I/M1), mica 2 (M2), quartz (Q), feldspar K (FK), plagioclase (P), hematite (He) and augite (A). **b)** Patterns of X-ray diffraction powders of five samples of bricks. The mineral phases identified are mica (M), amphibole (Hb), zeolite-like (Z), quartz (Q), feldspar K (FK), plagioclase (P), goethite (Go) and hematite (He).

Figure 8. Distribution of remnant magnetization – M_R vs. coercive field – H_C (M_R vs H_C). M_R is the remnant magnetization value after applied field H_{max} up to 300 mT; H_C is the corresponding coercive field.

Figure 9. a) Hysteresis loops at room temperature on as found samples from Andalusia (Spain): tile XIII and clay 11, b) variation of the magnetic parameters, magnetization *vs*. coercive field, as a function of the applied thermal treatment temperature, c) hysteresis loops after thermal treatment at 700 °C and 600 °C respectively on clay 11 and tile XIII samples, d) thermomagnetic curve up to 800 °C on tile XIII and clay 11 from, treated up to 800 °C.

Figure 10. a) Hysteresis loops at room temperature on as found samples from *Hasta* (ceramic VI) and Cellarengo (soil 8), b) variation of the magnetic parameters, magnetization *vs*. coercive field, as

a function of the applied thermal treatment temperature, c) hysteresis loops on as found sample VI and soil 8 after thermal treatment at 600 °C, d) thermomagnetic curve on sample VI and clay 8, treated at 600 °C and 700 °C respectively.

Figure 11. Magnetization curve of the archaeological tile IV (Brandizzo), as found, with stamp M•A• [H].

Figure 12. Patterns of X-ray diffraction powders of soil 5-Vauda heated up to 1100 °C. The mineral phases successively identified are: smectite (Sm), chlorite (Ch), mixed-layer (ML), illite (I), muscovite-like (M1), paragonite-like (M2), kaolinite (K) quartz (Q), feldspar K (FK), plagioclase (P), goethite (Go), hematite (He), magnetite (Mg) and mullite (Mu).

Figure 13. FTIR spectra. Bricks II-*Segusio* and VI-*Hasta* compared to their most probable source, soil 5-Vauda fired within the range of temperatures 680–1100 °C.

Figure 14. NIR spectra. **a)** Archaeological samples of four tiles and four bricks from the same site of sample XI-*Industria* compared to soil 5-Vauda fired at different temperatures. **b)** Soil 5-Vauda fired within the range of temperatures 680–1100 °C.

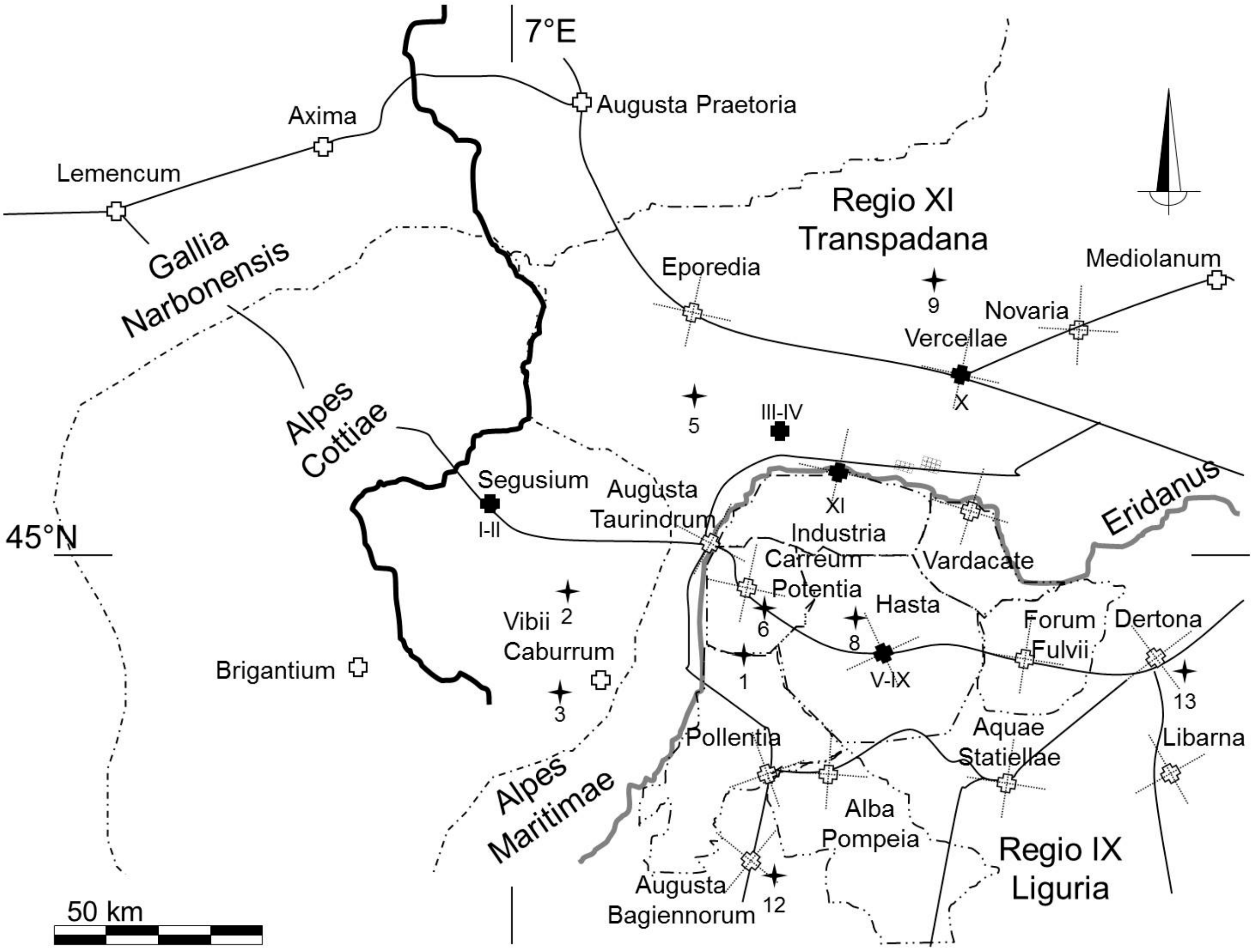
7°E
Augusta Praetoria
Axima
Lemencum
Gallia Narbonensis
Regio XI
Transpadana
Eporedia
Mediolanum
9
Novaria
Vercellae
X
5
III-IV
Alpes Cottiae
Segusium
I-II
Augusta
Taurindrum
XI
Eridanus
45°N
Industria
Carreum
Vardacate
Potentia
Hasta
Forum
Fulvii
Dertona
2
Vibii
Caburrum
6
8
V-IX
1
Brigantium
3
13
Aquae
Statiellae
Libarna
Pollentia
Alba
Pompeia
Alpes
Maritimae
Regio IX
Liguria
Augusta
Bagiennorum
12
50 km

Figure 1

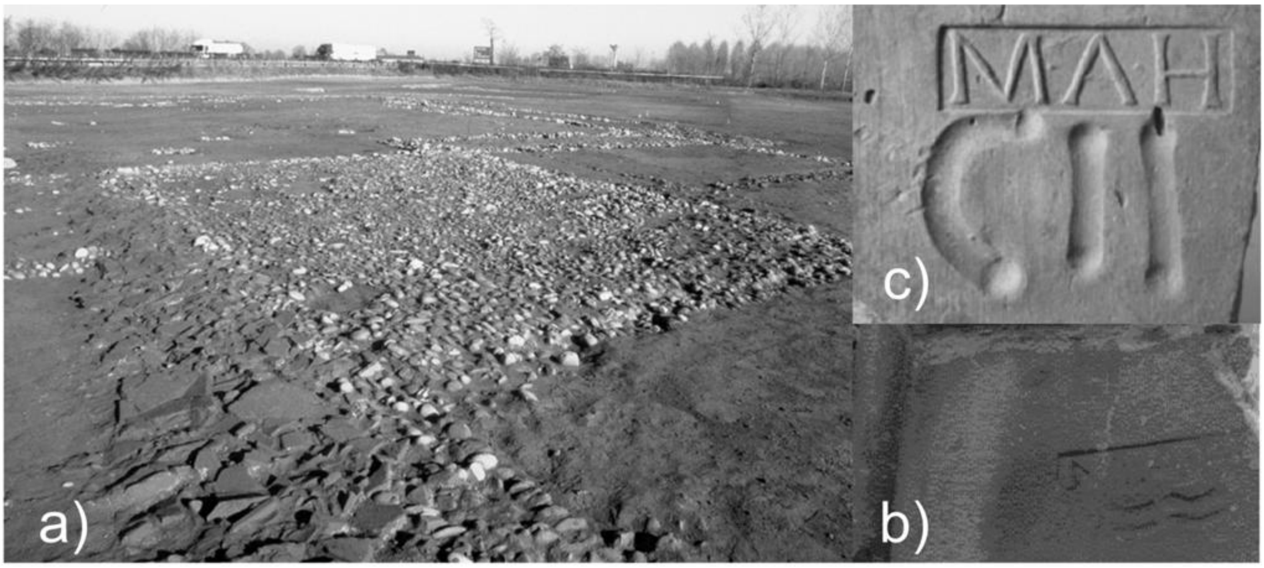

Figure 2

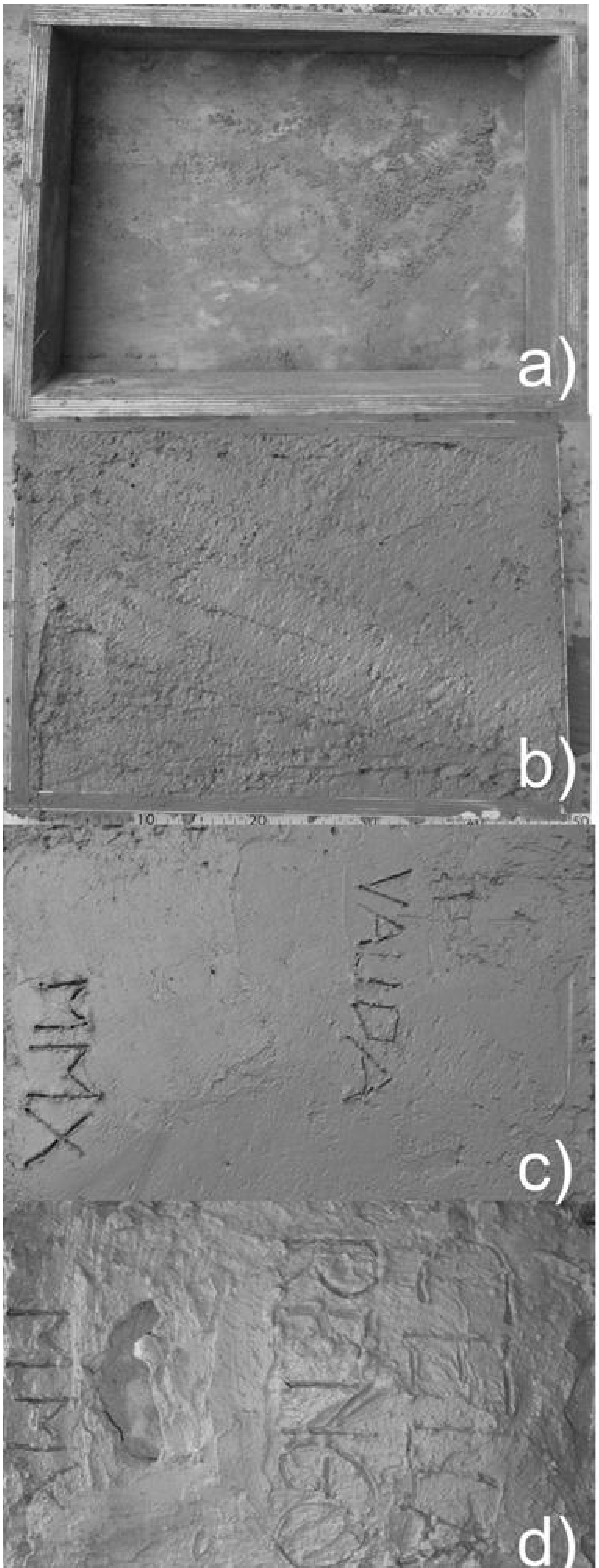

Figure 3a

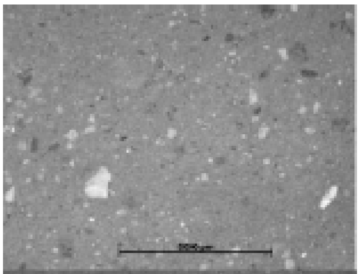	Fragment with parallel faces, fine paste, homogeneous, not abundant large air bubbles. Poorly sorted particles: pink and yellow tabular and cylindrical 20%, white subangular blocky (1 mm) 10%, rounded and sub-rounded tabular grey and white 5%.	**XI-IND01** 5YR 6/6 (reddish yellow) Q, FK, I, I/Sm, Hb, He, Go
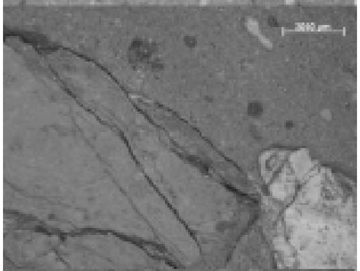	Fine paste packing small millimetrical granules black and white and grey areas, relatively frequent fine air bubbles. Unsorted particles: brown and yellowish cracked sub-angular lenticular (10 mm) 50%, sub-angular globular and lenticular pores 20%.	**XI-IND02** 5YR 6/8 (reddish yellow) Q, FK, I, Hb, I/Sm, Go, He
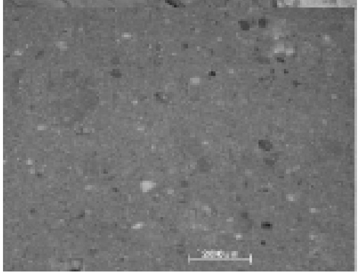	Curved fragment with parallel faces, fine paste embedding millimetrical black and white and gray areas (>IND02) and black granules coupled to rare and large air bubbles. Poorly sorted particles: pink and yellow tabular 20%, white subangular blocky 5%, sub-angular globular and lenticular pores 10%.	**XI-IND03** 5YR 6/8 (reddish yellow) Q, FK, I, Hb, I/Sm, Go, He
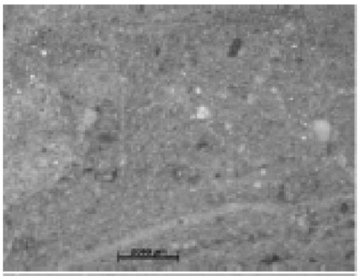	Fragment with parallel faces on one side white, granular (fine grain) with opaque white areas, not grey areas, rare very fine and elongated air bubbles. Poorly sorted and locally oriented particles: white angular tabular 20%, sub-angular globular and lenticular and cylindrical pores 20%.	**XI-IND04** 5YR 6/6 (reddish yellow) Q, FK, I, I/Sm, C, He, Hb
	Fine paste embedding sub-mm grains, white and opaque granules scarce, rare and small (few elongated) air bubbles. Moderately sorted and oriented particles: white angular tabular 20%, sub-rounded platy orange, yellow and white 10%, sub-angular globular and cylindrical pores 10%.	**XI-IND05** 2.5YR 5/6 (red) Q, FK, I/Sm, Ch, He, Hb, Go
	Massive fragment with parallel faces, oriented texture packing white, opaque and rarely black fragments, rare vacuolar air bubbles. A fractured rounded area and unsorted particles: sub-angular white tabular coloured in brownish and yellowish (2 mm) 5%, small yellow tabular 5%, sub-angular lenticular pores 20%.	**XI-IND06** 2.5YR 5/6 (red) Q, He, spinels
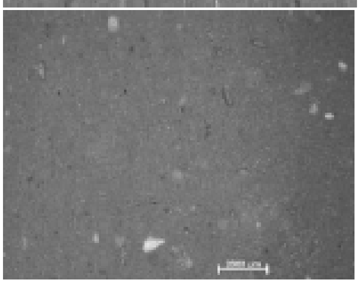	Solid rectangular block, fine paste with rare white, opaque and orange granules: black granules in the interior, white and larger outside. Few and large air bubbles. Unsorted particles: sub-angular white tabular 10%, yellow and white subangular blocky 5%, rounded globular lenticular pores 20%.	**XI-IND07** external 2.5YR 5/4 (reddish brown), external 10R 4/6 (red) Q, He, spinels

Figure 3b

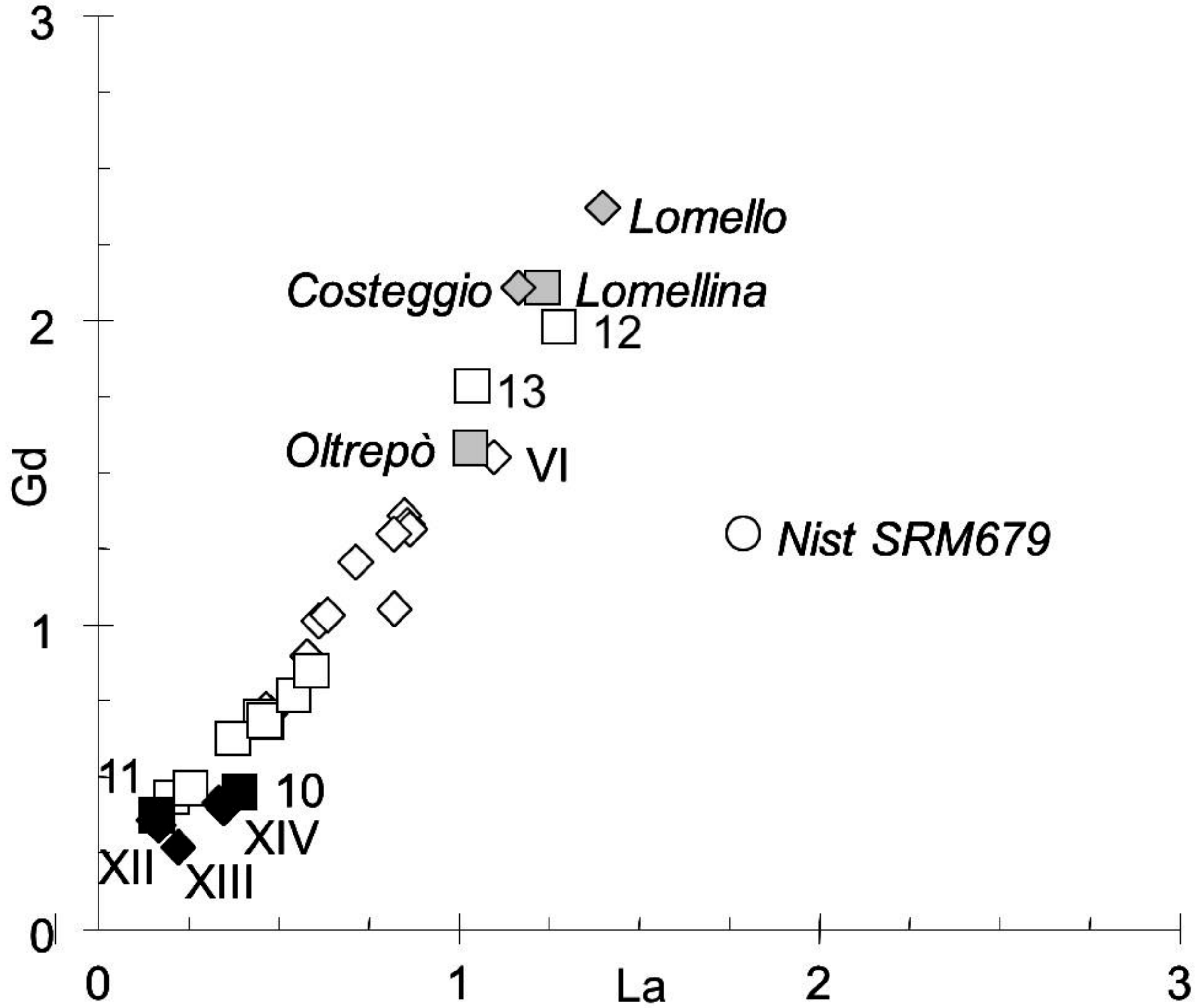

926

927 Figure 4

928

929

a)

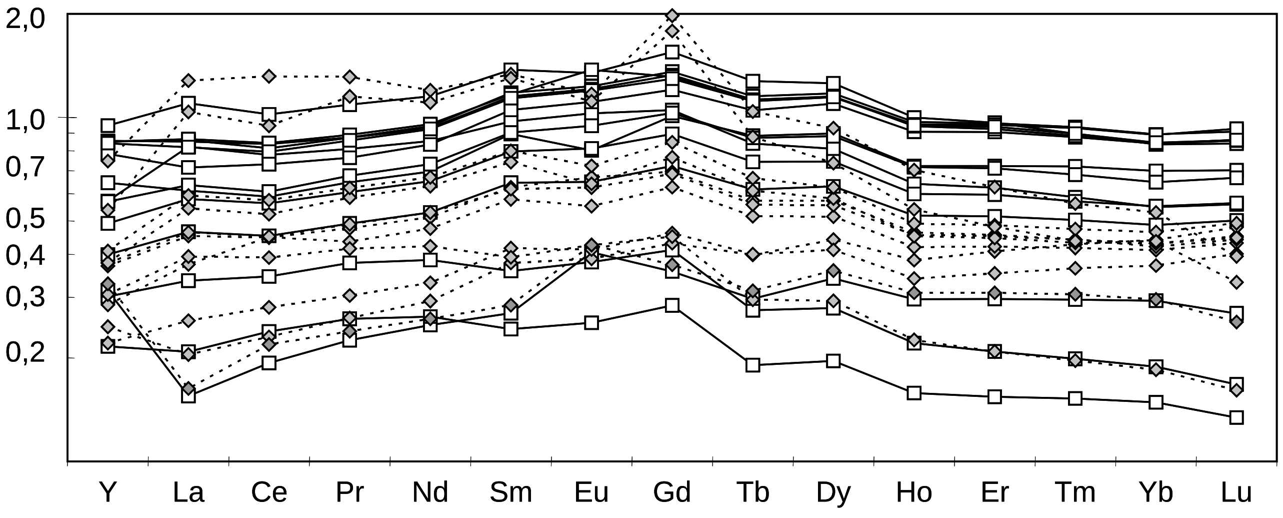

2,0
1,0
0,7
0,5
0,4
0,3
0,2
Y La Ce Pr Nd Sm Eu Gd Tb Dy Ho Er Tm Yb Lu

b)

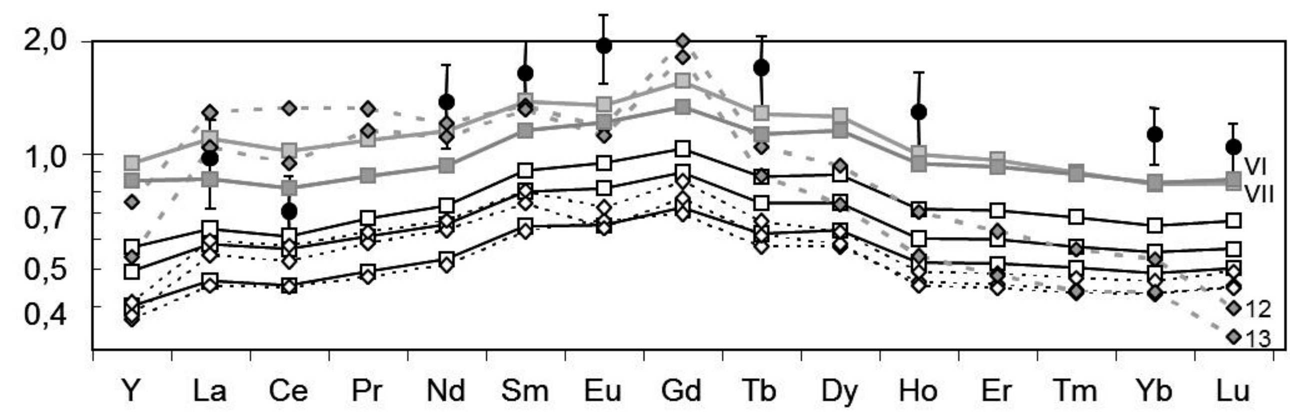

2,0
1,0
0,7
0,5
0,4
VI
VII
12
13
Y La Ce Pr Nd Sm Eu Gd Tb Dy Ho Er Tm Yb Lu

Figure 5

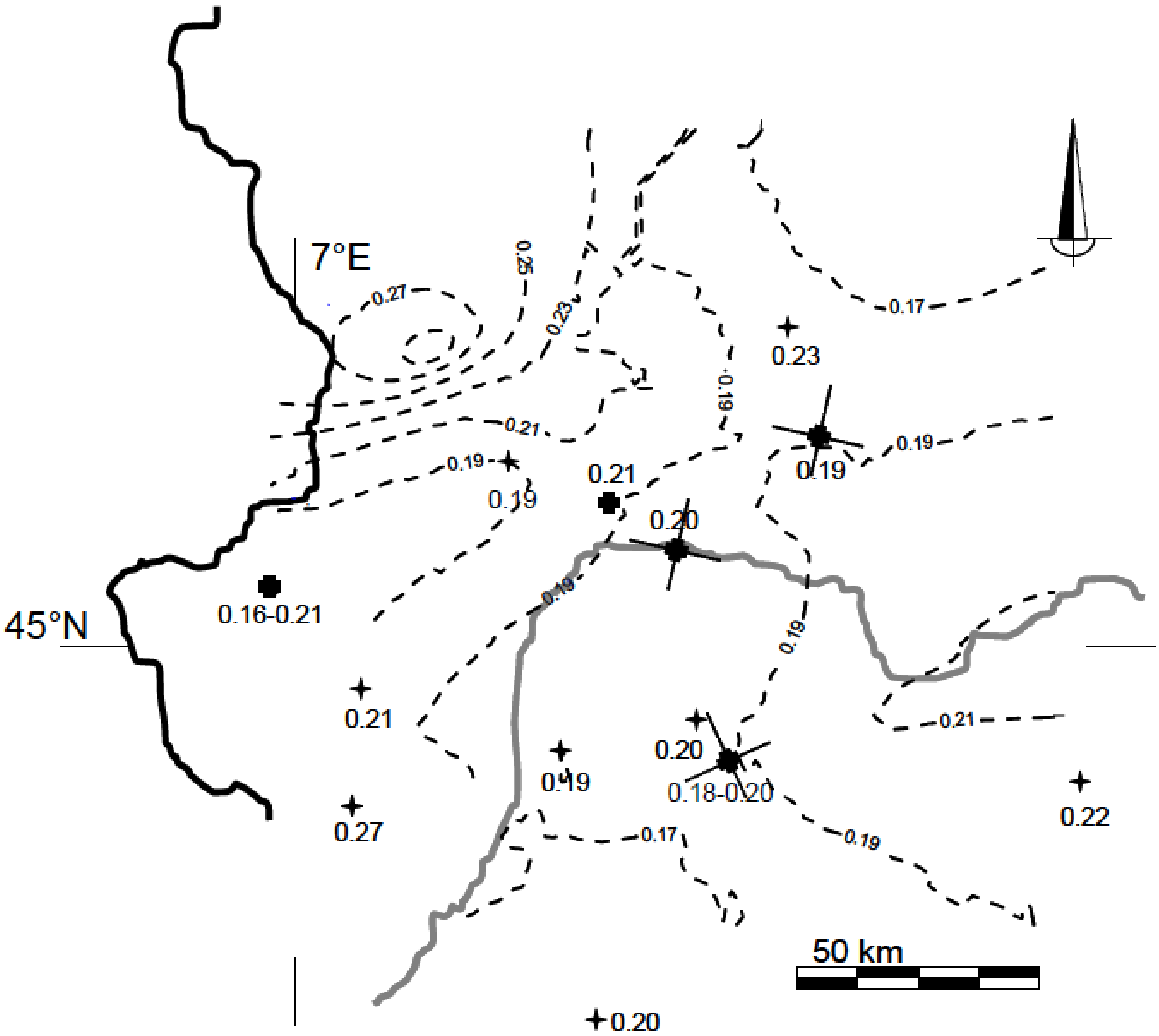

935

936 Figure 6

a)

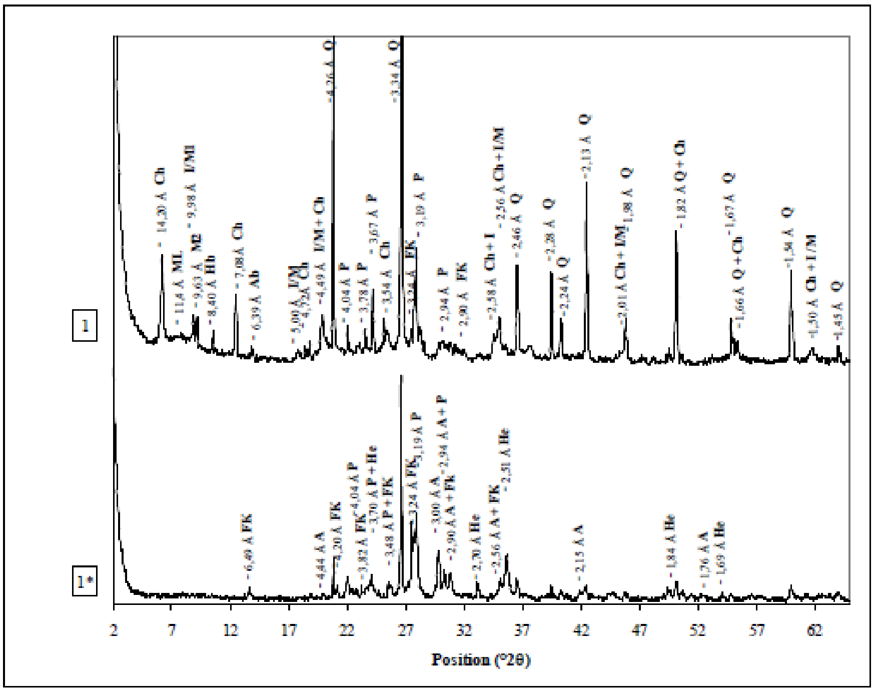
1
1*
2
7
12
17
22
27
32
37
42
47
52
57
62
Position (°2θ)

b)

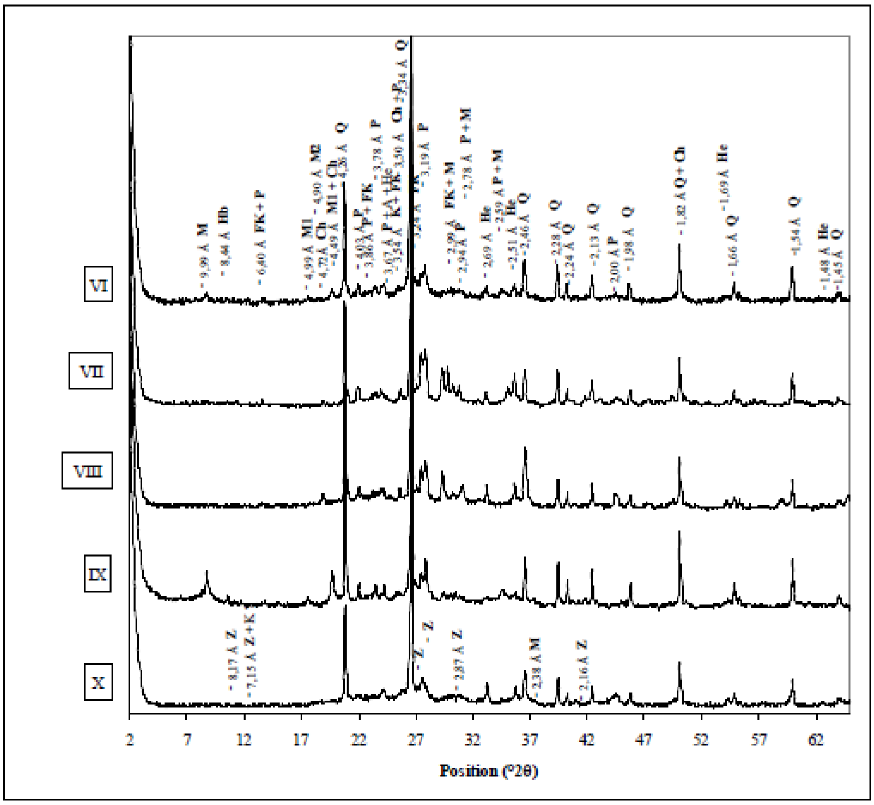
VI
VII
VIII
IX
X
2
7
12
17
22
27
32
37
42
47
52
57
62
Position (°2θ)

Figure 7

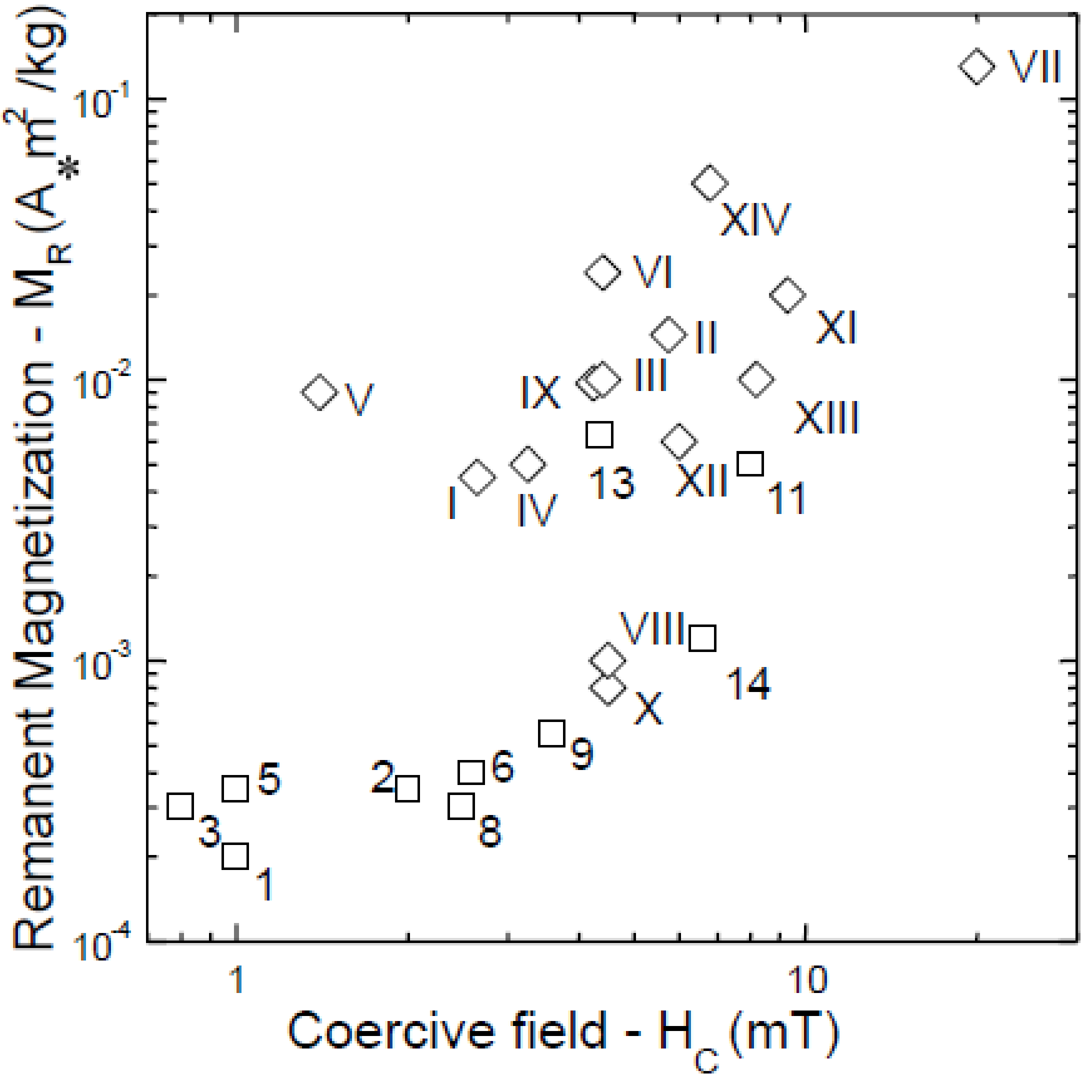
Remanent Magnetization - M_R (A*m^2 /kg)
Coercive field - H_C (mT)
10^-1
10^-2
10^-3
10^-4
1
10
VII
XIV
VI
XI
II
III
IX
V
XIII
13
XII
11
I
IV
VIII
14
X
9
6
5
2
3
8
1

Figure 8

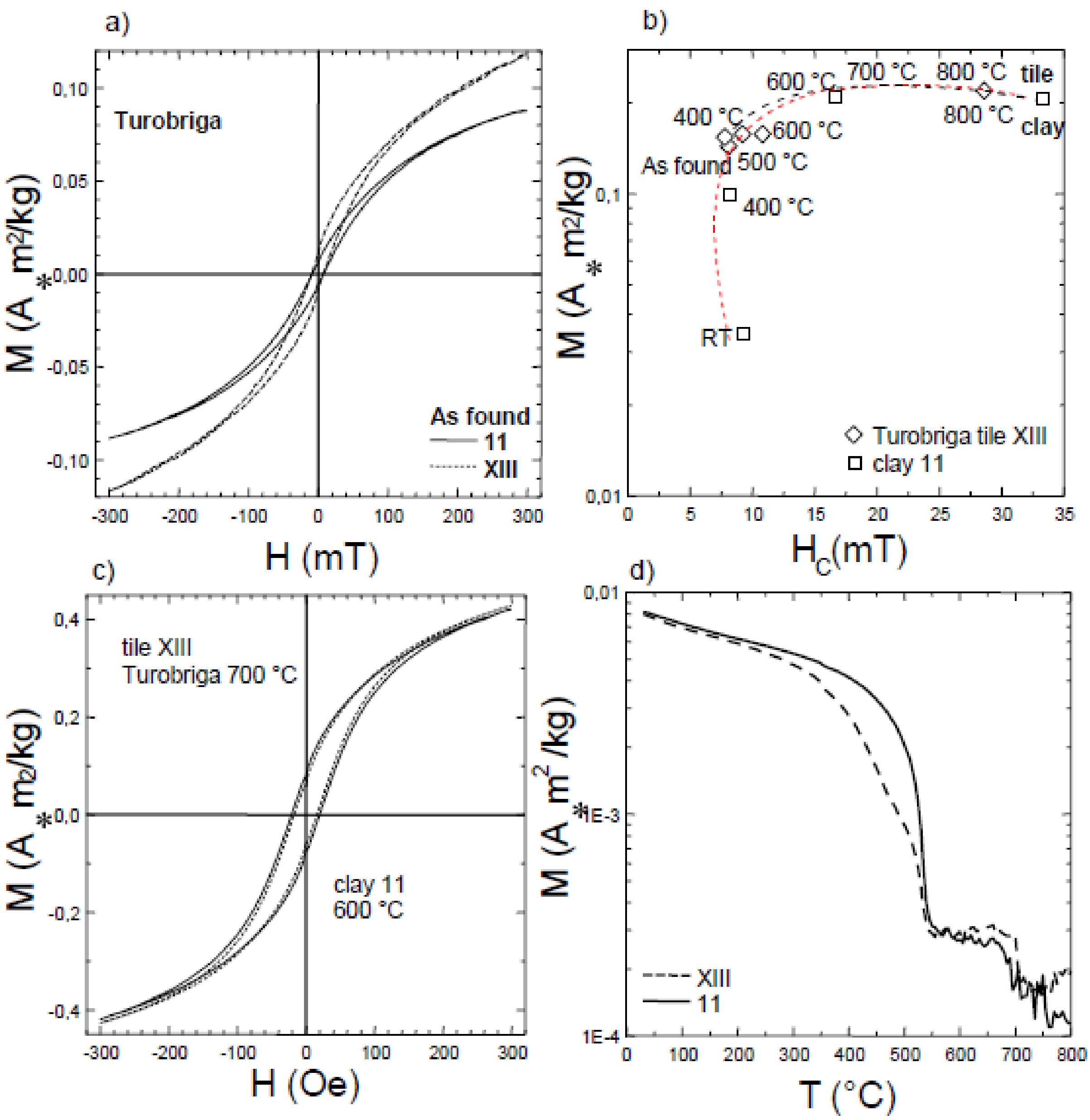

940

941 Figure 9

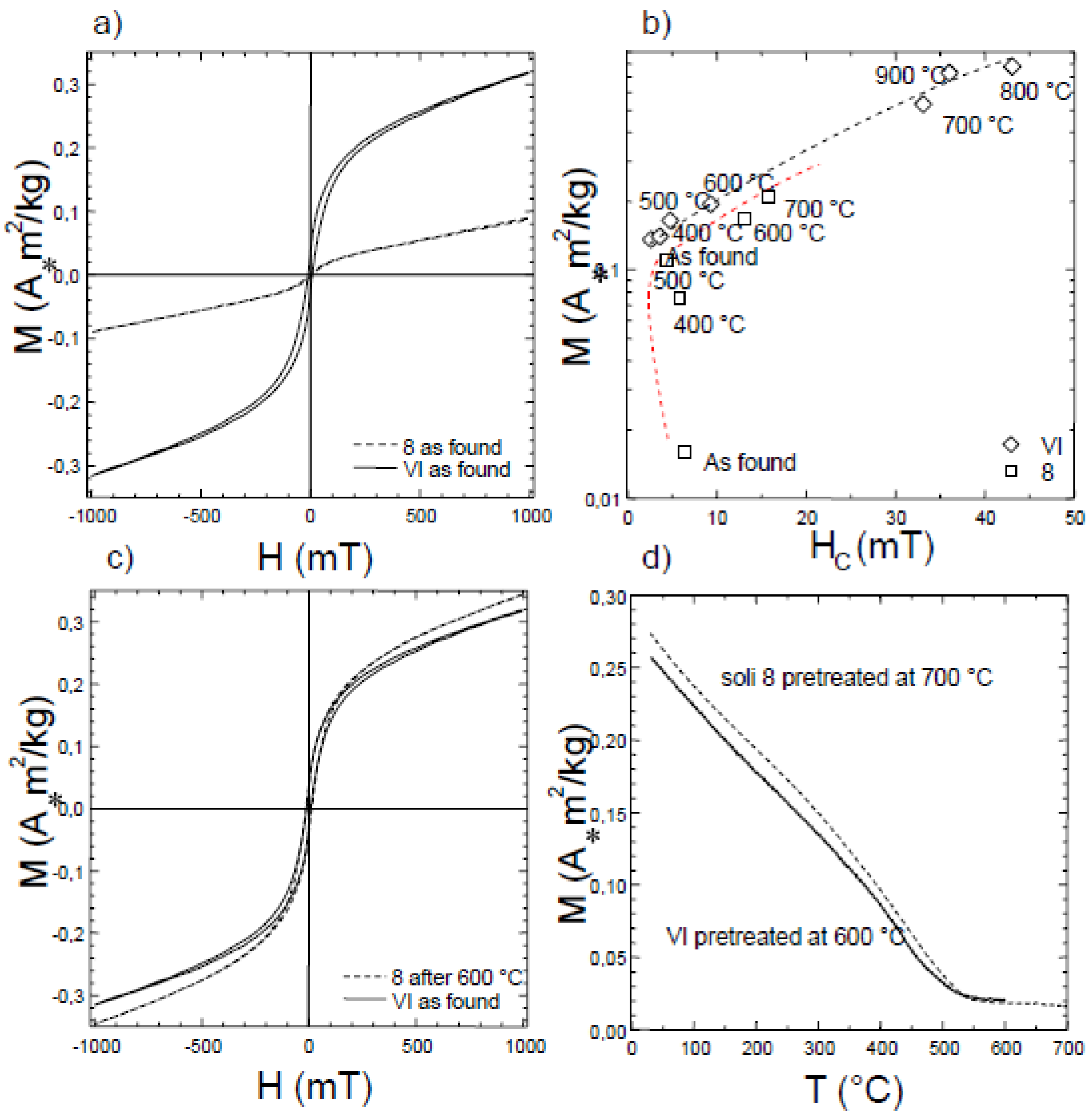
a)
b)
c)
d)
M (A*m²/kg)
H (mT)
H_C (mT)
T (°C)
8 as found
VI as found
8 after 600 °C
900 °C
800 °C
700 °C
600 °C
500 °C
400 °C
As found
VI
8
soli 8 pretreated at 700 °C
VI pretreated at 600 °C

Figure 10

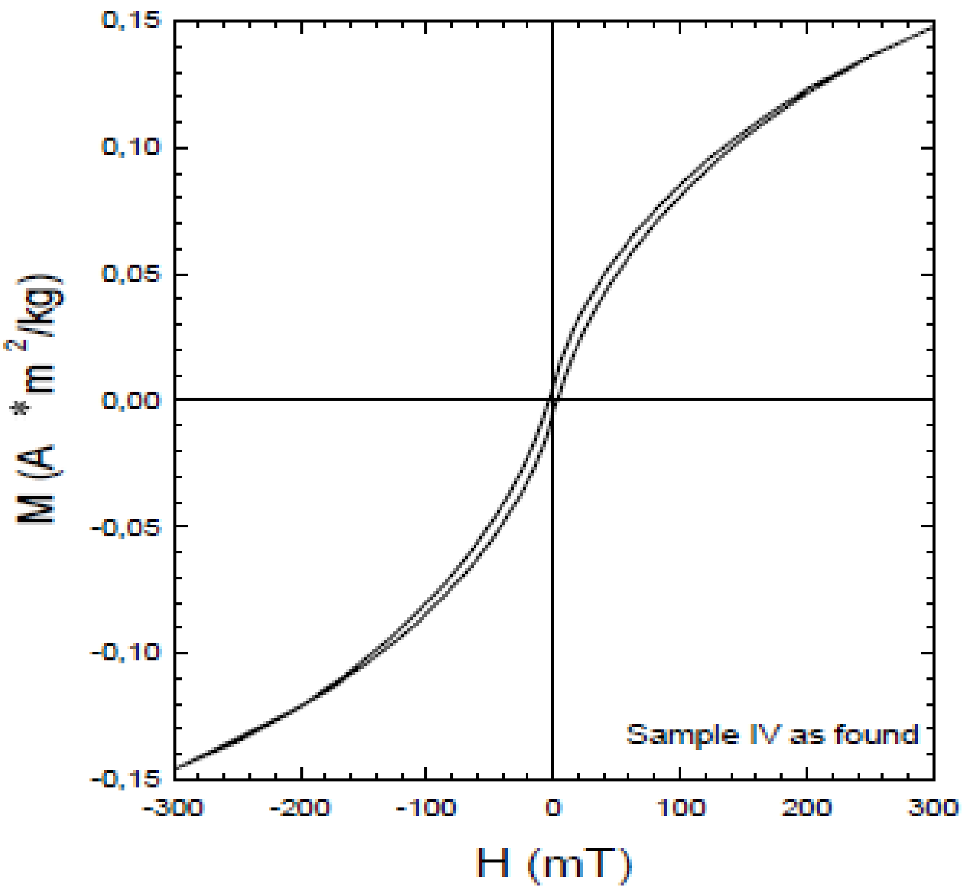
0,15
0,10
0,05
0,00
-0,05
-0,10
-0,15
M (A *m 2/kg)
-300
-200
-100
0
100
200
300
H (mT)
Sample IV as found

Figure 11

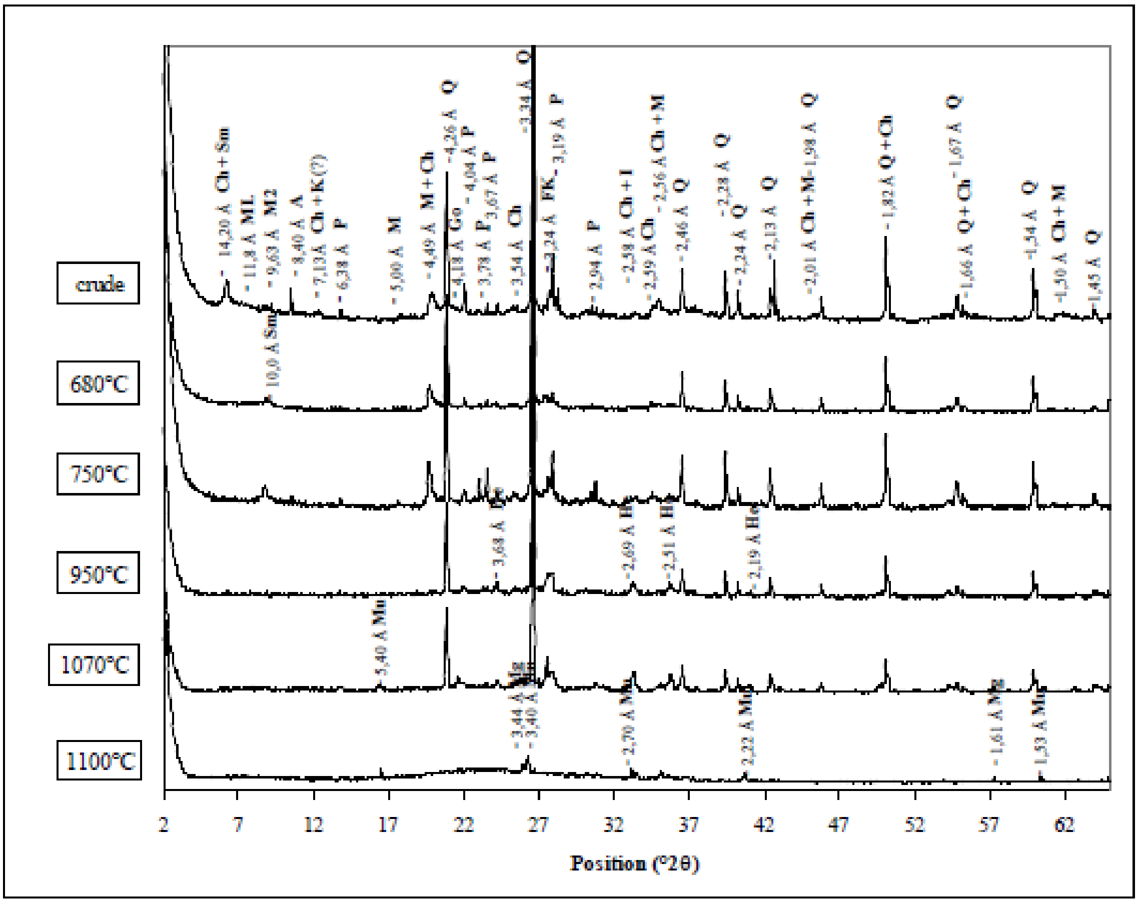
crude
680°C
750°C
950°C
1070°C
1100°C
2
7
12
17
22
27
32
37
42
47
52
57
62
Position (°2θ)

Figure 12

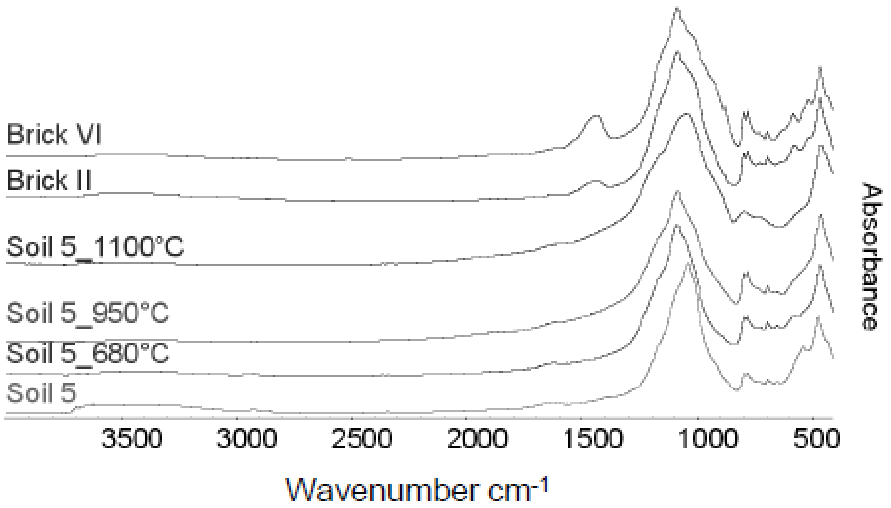
Brick VI
Brick II
Soil 5_1100°C
Soil 5_950°C
Soil 5_680°C
Soil 5
3500
3000
2500
2000
1500
1000
500
Wavenumber cm-1
Absorbance

Figure 13

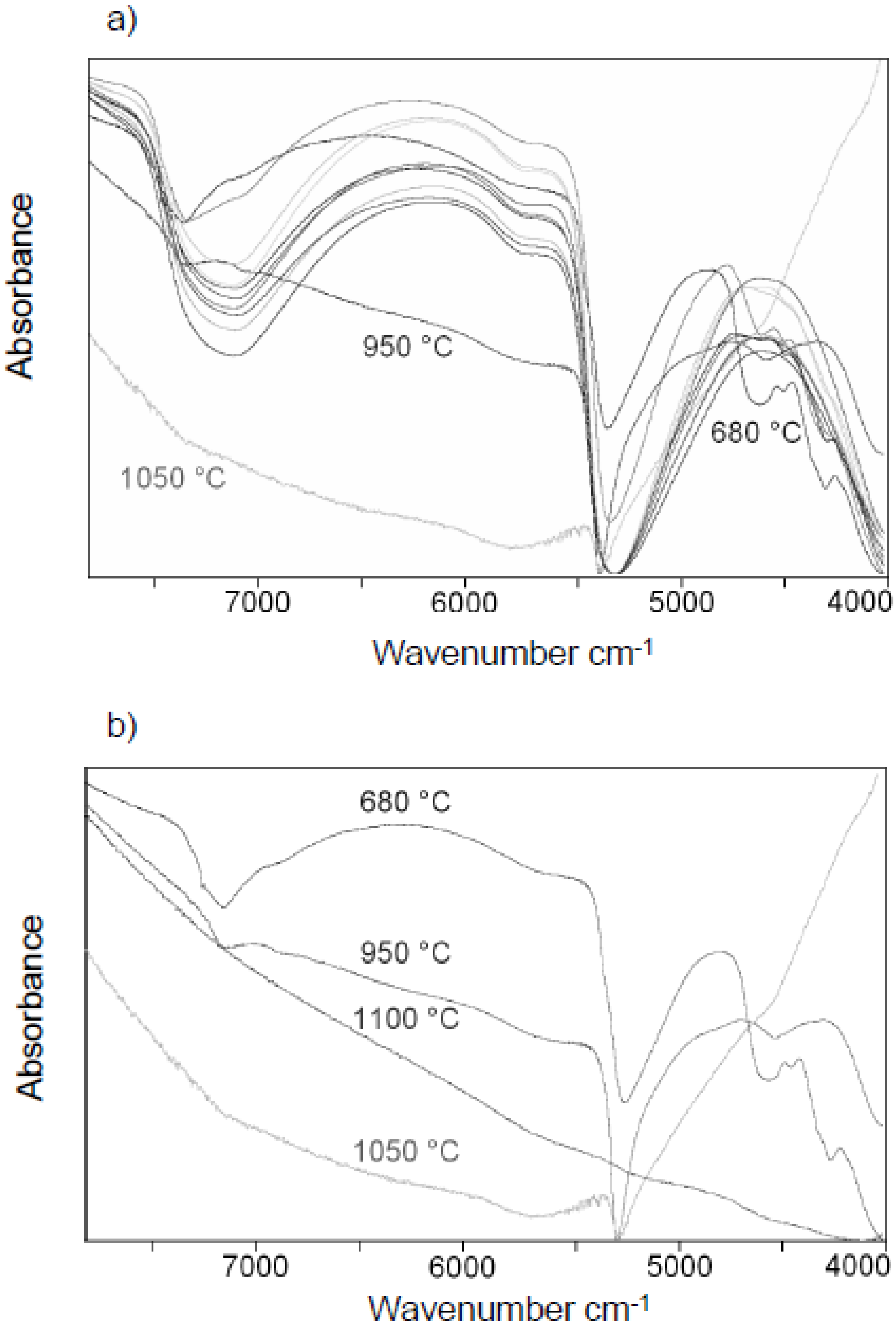
a)
Absorbance
950 °C
680 °C
1050 °C
7000
6000
5000
4000
Wavenumber cm-1
b)
Absorbance
680 °C
950 °C
1100 °C
1050 °C
7000
6000
5000
4000
Wavenumber cm-1

Figure 14

Table 1. Site data selected upon the localities of archaeological samples (✦ in Figure 1).

soil	site	coordinates	former *Regio*	soil taxonomy[a]	sequence of horizons	clay	$CaCO_3$	skeleton
						--------	percent	-----------
1	Poirino	44°5′N 7°51′E 177 m a.s.l.	IX *Liguria* (LI)	Typic Haplustalf	Ap-AB-Bt1-Bt2	>25	0	0
2	Piscina	44°55′N 7°26′E 288 m a.s.l.	*Alpes Cottiae* (CA)	Typic Hapludalf	Ap-Bt1-Bt2-BCt	>20	0	50[2]
3	Bagnolo	44°46′N 7°19′E 358 m a.s.l.	*Alpes Cottiae* (CA)	Typic Fraglossudalf	A-E-E/B-Btx	>40	0	0
5	Vauda	45°17′N 7°37′E 380 m a.s.l.	XI *Transpadana* (TP)	Typic Fragiudalf	A-E-Btx1-Btx2	>20	0	0
6	Chieri	44°59′N 7°52′E 276 m a.s.l.	IX *Liguria* (LI)	Inceptic Haplustalf	A-E/Bt-Bt1-Bt2	>20	0	0
8	Cellarengo	44°51′N 7°55′E 320 m a.s.l.	IX *Liguria* (LI)	Typic Haplustalf	Ap-E-Bt1-Bt2-Btg	>20	0	0
9	Rovasenda	45°32′N 8°19′E 220 m a.s.l.	XI *Transpadana* (TP)	Aquic Fraglossudalf	Ap-E-Btg1-Btg2- Btc	>30	0	0
10	Bujalance	37°53'N 4°23'W 357 m asl	*Hispania Baetica* (HB)	Vertic Xerochrepts	A-Bc-Bck	>40	>5	0
11	Aroche	37°56'N 6°57'W 420 m asl	*Hispania Baetica* (HB)	Calcic Haploxeralf	A-Bt-BCck	>40	>5	0
12	Bene Vagienna	44°33’N 7°50’W 350 m a.s.l.	IX *Liguria* (LI)	Typic Paleustalf	A-E-Bt-2Bt-3Bt	>30	0	0
13	Tortona	44°53’N 8°51’W 122 m a.s.l.	IX *Liguria* (LI)	Typic Haplustalf	Ap1-Ap2-Bt1-Bt2	>30	20[1]	0

[a]The taxonomy (Soil Survey Staff, 1999) used in surveys and mapping at the regional level, to facilitate the comparison we have decided neither to update nor to convert to other taxonomic systems. All soils are mixed, nonacid, mesic, their particle size distribution spans from fine-silty, fine-loamy, to loamy (URL www.regione.piemonte.it/agri/area_tecnico_scientifica/suoli/dati.htm).

[1] >150 cm; [2] >120 cm

Table 2. Archaeological bricks and tiles (✚ in Figure 1)

brick	site	coordinates	*Regio*	site	type	epoch[a]
I	*Segusio*	45°8′N 7°3′E 503 m a.s.l.	*Alpes Cottiae* (CA)	*domus* - tile fall	tile	I-III c. AD
II	*Segusio*	idem	*Alpes Cottiae* (CA)	*domus* – sporadic within the layer	brick	I-III c. AD
III	Brandizzo	45°11′N 7°50′E 187 m a.s.l.	XI *Transpadana* (TP)	*villa rustica* – tile fall	tile	I-II c. AD
IV	Brandizzo	idem	XI *Transpadana* (TP)	*villa rustica* – tile fall	tile, stamp M·A·[H]	I-II c. AD
V	*Hasta*	44°53′N 8°12′E 123 m a.s.l.	IX *Liguria* (LI)	Brick (kiln?)	brick	I-II c. AD
VI	*Hasta*	idem	IX *Liguria* (LI)	public building wall (positioning floor levelling course)	brick	first half I c. AD
VII	*Hasta*	idem	IX *Liguria* (LI)	main sewer conduct under *decumanus*	sewerage brick	I c. BC
VIII	*Hasta*	idem	IX *Liguria* (LI)	clay pipe conduct under *decumanus*	*tubulus*	I-II c. AD
IX	*Hasta*	idem	IX *Liguria* (LI)	clay pipe conduct under *decumanus*	*tubulus*	I-II c. AD
X	*Vercellae*	45°19′N 8°25′E 130 m a.s.l.	XI *Transpadana* (TP)	amphitheatre foundation bedplate (outer ring)	brick	II c. AD
XI	*Industria*	45°11′N 7°58′E 177 m a.s.l.	IX *Liguria* (LI)	Isis temple podium (levelling course)	brick	I c. AD
XII	*Bujalance*	37º55'N 4º22'W 360 m a.s.l.	*Hispania Baetica* (HB)	Not determined	tile	I c. AD
XIII	*Turóbriga*	37°58'N 6°56'W 270 m a.s.l.	*Hispania Baetica* (HB)	*thermae* – public baths	tile (XIIa), brick (XIIb)	I c. AD
XIV	*Itálica*	37°26′N 6°02′W 18 m a.s.l.	*Hispania Baetica* (HB)	Not determined	tile	II c. AD

[a]Dating (in centuries) have been made from the archaeological record by a direct study of artefacts deduced by association with other materials found in the context and inferred by their point of discovery in the sequence relative to datable contexts

Table 3. REY in archaelogical bricks and tiles. Unit: μmol kg^{-1}.

	I *Segusio*	II *Segusio*	III Brandizzo	IV Brandizzo	V *Hasta*	VI *Hasta*	VII *Hasta*	VIII *Hasta*	IX *Hasta*	X *Vercellae*	XI *Industria*	XII *Bujalance*	XIII *Turòbriga*	XVI *Itàlica*
Y	160	141	194	211	99	234	210	141	122	210	208	75	78	53
La	132	177	154	184	100	237	185	137	125	187	177	72	33	45
Ce	269	355	334	382	207	466	371	278	257	385	363	157	88	109
Pr	33	41	38	44	25	55	44	34	31	45	43	19	11	13
Nd	125	154	150	170	95	208	168	132	118	172	167	69	45	47
Sm	27	29	31	35	19	41	34	27	24	35	34	11	8	7
Eu	5	6	6	7	4	8	7	5	5	8	7	2	2	1
Gd	24	25	29	33	17	37	32	25	22	32	31	10	9	7
Tb	4	3	4	5	2	5	4	3	3	4	4	1	1	1
Dy	19	17	24	25	14	27	25	19	16	25	25	6	7	4
Ho	3	3	4	5	2	5	5	3	3	5	5	1	1	1
Er	10	9	12	13	7	13	13	10	8	13	13	3	4	2
Tm	1	1	2	2	1	2	2	1	1	2	2	0	1	0
Yb	9	7	11	11	6	11	11	8	7	11	11	2	4	2
Lu	1	1	2	2	1	1	2	1	1	2	2	0	0	0
$\Sigma LREE_{UCC}$	5	6	6	7	4	8	7	5	4	7	7	2	2	2
$\Sigma HREE_{UCC}$	6	6	8	8	4	9	8	6	5	8	8	2	2	1
$(Gd/La)_{UCC}$	1.6	1.3	1.7	1.6	1.6	1.4	1.5	1.6	1.5	1.5	1.6	1.2	2.3	1.4

Table 4. Matching table. Roman bricks *vs* most probable soils utilised as raw material based on the REY_{UCC} pattern. Matching shown only matches where their individual probability is associated with a two-tailed heteroscedastic Student *t* test >0.58, if the most probable distance by Roman roads was <100 km.

Archaeological artefact	Raw soil
I-*Segusio*	3-Bagnolo 6-Chieri 8-Cellarengo 9-Rovasenda
II-*Segusio*	1-Poirino
III-Brandizzo IV-Brandizzo V-*Hasta* VIII-*Hasta* IX-*Hasta* XI-*Industria*	5-Vauda
X-*Vercellae*	1-Poirino 3-Bagnolo 5-Vauda

Table 5. XRD bricks and tiles.

Artefact		colour[a]	Q[b]	FK	P	Hb	V	Sm	Ch	M1	M2	I	Ho	Go	He	Ca	Do	Ge	Py	Mu
I	*Segusio*	5YR 7/4	+++	++	+	(+)				+				(+)	+					
II	*Segusio*	5YR 6/6	+++	+	++									+	++					
III	Brandizzo	2.5YR 6/8	+++		++	(+)									++					
IV	Brandizzo	5YR 6/8	+++	+	+	+									+					
V	*Hasta*	5YR 6/6	+++	+	+					+					+					
		5YR 8/6																		
VI	*Hasta*	5YR 8/3	+++	++	+										+	+	(+)		(+)	
		7.5YR 8/6																		
VII	*Hasta*	7.5YR 7/6	+++	+	+										+	(+)				
VIII	*Hasta*	2.5YR 4/4	+++	+	+	(+)				(+)		(+)			+					
IX	*Hasta*	2.5YR 5/4	+++	+	+										++					
X	*Vercellae*	10R 5/8	+++	++	+	+				+					+					
XI	*Industria*	5YR 6/6	+++	+	+	+									+					
XII	*Bujalance*	2.5YR 8/4	+++	(+)	(+)										(+)	++		+		
XIII	*Turóbriga*	7.5YR 4/6	+++	(+)	(+)					+					(+)	++				
XIV	*Itálica*	7.55YR 7/8	+++	(+)	(+)					(+)					(+)	++				

[a] colour zoning from the rim towards the center of the brick ot tile

[b] Q (quartz), FK (K-feldspath), P (plagioclase), Hb (amphibole), V (vermiculite), Sm (smectite), Ch (chlorite), M1 (muscovite-like), M2 (paragonite-like), I (illite), Ho (hornblende), Go (goethite), He (hematite), Ca (calcite), Do (dolomite), Ge (gehlenite), Py (pyroxene), Mu (mullite). In parenthesis poorly crystalline phases, bold high crystallinity.

Table 6. XRD soil 5-Vauda within the range of temperatures 680-1100 °C

Temp /°C	t /hr	Atm[a]	color	Q[b]	FK	P	F	Hb	Sm	Ch	M1	M2	I	Ho	Go	He	Ca	Do	Ge	Py	Mu
60	12	ox	10YR 6/4	+++	++	++			(+)	++	+	+	(+)		(+)						
680	6	ox	2.5YR 5/8	+++	+	+			(+)	(+)	(+)	(+)	(+)			(+)					
750	12	ox	2.5YR 5/8	+++	+	+										+					
950	4	ox	2.5YR 5/8	+++	+	(+)										+					(+)
1070	2	ox	10R 4/6	++			(+)									+					+
1100	12	red	7.5YR 2/1	*												+					++

[a] Atm, atmosphere. ox, oxidising; red, reducing atmosphere obtained by OM rich bricks according to Wolf (2002)

[b] Q (quartz), FK (K-feldspath), F (exsolution feldspars), P (plagioclase), Hb (amphibole), Sm (smectite), Ch (chlorite), M1 (muscovite-like), M2 (paragonite-like), I (illite), Ho (hornblende), Go (goethite), He (hematite), Ca (calcite), Do (dolomite), Ge (gehlenite), Py (pyroxene), Mu (mullite). (*) vitreous phase. In parenthesis poorly crystalline phases, bold high crystallinity.

Table 7. Temperature thresholds of decompositions and neoformations**.** Mineral neoformation (empty histograms, mineral in italics), beginning of instability (bars, minerals in bold), and some Curie temperatures (T_C). Scale in Celsius degrees.

Mineral	300 400 500 600 700 800 900 1000 1100 1200	Reference[b]
C disappearance from labile organic matter		1
structural H_2O disappearance		1
αFeOOH (goethite)		2, 3
δFeOOH (feroxyhite)		2, 4
γFe_2O_3 (maghemite) *γFe_2O_3 (maghemite)*	T_C	3, 5
Fe_3O_4 (magnetite)	T_C	2, 6
αFe_2O_3 (hematite)	T_C	7, 8, 9
Mg,Fe)$_3$(Si,Al)$_4$O$_{10}$(OH)$_2$·(Mg,Fe)$_3$(OH)$_6$ (Fe-rich chlorites)		10
$CaCO_3$ (calcite)[a]		6, 11
(Mg,Fe)$_3$(Si,Al)$_4$O$_{10}$(OH)$_2$·(Mg,Fe)$_3$(OH)$_6$ (Mg-rich chlorites)		10
(K,H$_3$O)(Al,Mg,Fe)$_2$(Si,Al)$_4$O$_{10}$[(OH)$_2$,(H$_2$O)] (illite)		10, 18
$Al_2Si_2O_5(OH)_4$ (kaolinite)		1, 12
(K,Na)(Si,Al)$_4$O$_8$ (sanidine)		6
Mg_2SiO_4 (forsterite)		6
$Ca_2Al[AlSiO_7]$ (gehlenite)		6, 11, 20, 21
$MgCaSi_2O_6$ (diopside)		11, 20
γAl_2O_3 (spinel)		10
(Mg,Fe)$_2$SiO$_4$ (olivine)		10, 13
$CaAl_2Si_2O_8$ (anorthite)		1
SiO_2 (tridymite)		1
SiO_2 (cristobalite)		1
Mg, Fe SiO$_6$ (pyroxenes)		13
(Na,Ca)$_{0,3}$(Al,Mg)$_2$Si$_4$O$_{10}$(OH)$_2$·n(H$_2$O) (montmorillonite)		14
$Al_2Si_2O_3$ (mullite)		1, 12, 14, 15
$CaSiO_3$ (wollastonite)		1, 6
	300 400 500 600 700 800 900 1000 1100 1200	

[a] thermodynamically a $\Delta G^{\circ} = 0$ of the reaction $CaCO_3(s) \rightarrow CaO(s) + CO_2(g)$ would occur at 833 °C

[b] references: 1) Velde and Druc (1999), 2) Schwertmann and Cornell (2000), 3) López et al. (2008), 4) Weckler and Lutz (1998), 5) Gendler et al. (2005), 6) Rathossi and Pontikes(2010), 7) De Boer and Dekkers (2001), 8) Morris (1994), 9) Zdujic et al. (1998), 10) Khalfaoui and Hajjaji (2009), 11) Lopez-Arce and Garcia-Guinea (2005), 12) Murad and Wagner (1991), 13) Echajia et al. (2006), 14) Rye (1981), 15) Rice (1987), 17) Dunlop (1997), 18) Cultrone et al. (2011), 19) Benea et al. (2010), 20) Maniatis et al. (1983), 21) Setti et al., 2006)

Table 8. Brickmaking. Effectiveness of analytical techniques compared by groupings: archeological methods (ARCHEO), routine methods (ROUTINE), mineralogy and spectroscopy (MIN), magnetic (MAG), metals (MET), and Rare Earth Elements and yttrium (REY).

Type of technique[1]		Origin of raw material[2]	Clues on technology[2]
ARCHEO†	Epigraphy	■	●
	Prosopography	■	●
	experimental archeology	■	●
	Shape	■	●
	Size	■	●
	Colour	■	●
	Stamps	■■■	●
ROUTINE	soil in field	□	●●
	chemical analyses	■	●
	physical analyses	■■	●●
	OM	■	●●
	LOI	■	●
MIN	XRD	■	●●
	FTIR	■	●●
	DRIFT	■■	●●
	SEM-EDS	■	●●
	XRF	■■	●
	Raman spectroscopy	■	●●
MAG	magnetization curves	■	●●●
	saturation magnetization	■	●●
	remanence	■	●●
MET	AAS	■■	○
	ICP-MS	■■	○
	EDAX	■■	○
	TOF-SIMS	■	●
REY	ICP-MS	■■■■	○○

[1] Optical microscopy **OM**, loss on ignition **LOI**, X-ray diffraction **XRD**, Fourier transform infrared spectroscopy **FTIR**, diffuse reflectance infrared Fourier transform spectroscopy **DRIFT**, scanning electron microscopy with energy dispersive spectrometer **SEM-EDS**, X-ray fluorescence **XRF**, atomic absorption spectroscopy **AAS**, inductively coupled plasma mass spectrometry **ICP-MS**, time-of-flight secondary ion mass spectrometry **TOF-SIMS**, energy dispersive spectrometer **EDAX**

[2] ■/●fair, ■■/●● moderate, ■■■/●●●effective, ■■■■/●●●● very effective [open symbols means without evidence in the current Literature]

† The bricks are extremely standardized, ubiquitous materials and very 'trivial' from an archaeological point of view. Very rare are the stamped bricks or tiles.

Supplementary Informations

Table SI1. Element concentrations in archaeological samples. Unit: μmol kg^{-1}.

	I *Segusio*	II *Segusio*	III Brandizzo	IV Brandizzo	V *Hasta*	VI *Hasta*	VII *Hasta*	VIII *Hasta*	IX *Hasta*	X *Vercellae*	XI *Industria*
Sc	8720	8493	8764	11007	7126	8305	9608	8715	6408	10010	8699
Ti	63772	94066	96040	87565	79733	73045	78402	88631	94270	95288	811279
V	1495	2147	1801	1800	1820	1485	1866	1991	2143	1729	16829
Cr	2117	3585	7025	8778	3254	1908	3336	3124	3085	2564	4500
Mn	28145	31026	15873	16992	11114	9597	15149	11272	9388	18658	13825
Fe	619849	730905	740440	805704	536724	495498	614746	620520	625757	687933	667252
Co	324	550	464	533	272	276	327	298	314	380	372
Ni	1455	2510	4837	5556	1521	883	1850	1768	1640	1229	2504
Cu	582	1027	601	657	323	324	416	494	434	376	481
Zn	1507	1781	1641	1620	1493	1158	1888	1534	1514	1370	2410
Sr	988	1295	895	943	880	2498	1511	1131	955	3544	1472
Mo	1	2	2	1	8	2	3	4	6	3	2
Pb	193	175	91	857	119	133	91	118	124	129	187
Th	342	390	380	437	205	521	436	279	258	604	364

Appendix. Size of Roman bricks

In general, bricks are small, rectangular and cubit square and very durable blocks of ceramics used for building. The dimensions of Roman bricks, expressed as multiples of the Roman foot unit (~ 30 cm), were equal to 1.5 feet (length) per 1.0 foot (width), with thickness up to 1.3 feet. In antiquity, they are commonly considered to have been obtained from selected soils, by mixing mud with straw, twigs, and/or dung that were subsequently either dried or fired (Dobson, 1850; Ducati, 1927). Normally, bricks are distinct from other stoneware because in their case, when fired, the components of clay usually do not reach as high temperature as to vitrify and remain porous. In addition, due to the plasticity of clay when sufficiently wet, bricks, before heating, can be easily manipulated to any desired shape (Pollard and Heron, 2008). In its treatise *De Architectura*, dated to the first century BC, the Roman writer and engineer Marcus Vitruvius Pollio sorted building materials into *lateres* (bricks), *harena* (sand), *calx* (limestone), *lapis* (stone), and *materies* (wood). Unfortunately, about brick technology Vitruvius only wrote that both typologies were in use, namely: *lateres*, for sun dried bricks and *lateres cocti* or *testacei*, for fired bricks. He added that bricks were mainly employed for facing purposes, and that tiles were often imitated by portions of *amphorae* and ceramics. At the same period associated with *caementum* (concrete), bricks became the building material most in use to erect weight-bearing structural parts (Coarelli, 2000). Although Vitruvius brought us scarce data on the manufacture of bricks, he held the idea that in each region of the Roman Republic the local sources should be preferred for building, implicitly confirming that brick production was a very large industry in the Roman *Regiones*, even when compared to modern standards (Helen, 1975). The use of bricks increased in Roman times throughout the second and first century BC, but nowadays almost nothing has remained of the many thousands of Roman houses built in the last period of the Republic and in the first part of the Empire. This scarcity largely depends on the refurbishment of Roman bricks that took place since the Middle ages, when the building materials locally available were exploited for secondary applications (Goll, 2005). Also, information on the building methods and resources used is very scarce. In the case of bricks, the origin of raw materials and the technology applied to brick-making have rarely been goals of research even in well-known historical contexts (Calliari et al., 2001; López-Arce et al., 2003). On the contrary, the firing behaviour of minerals in stoneware and in ceramics in particular has largely been investigated (e.g. Meloni et al., 2000; Rice, 1987), as well provenance studies of fine ceramics have been consolidated in the last decades, e.g. through trace element chemical analysis (Hatcher et al., 1994; Mirti et al., 1990; Marengo et al., 2005). Although the composition of fine pottery can differ from the clay it was made of, due to refinement processes employed to enhance mechanical resistance and sintering processes, this is not the usual case of raw building materials as tiles and bricks, upon which we have focussed our study.

Bricks for public buildings were employed mainly in city walls, towers and doors, but even in large bolster works of public buildings (temples, porticoes,...) and somewhere reinforcing private thin walls, barrel vaults of aqueducts – as introduced by military experts (Lancaster, 2010), – and later sanitary sewers. Outside of urban centers, bricks were used mainly in roofing (tiles) and foundations of villa urbana (country houses built for privileged classes) and villa rustica (farm-houses estate). The first city of Northern Italy surrounded by a defensive wall was Ravenna. In NW Italy, typically a city wall (height 2.4 m and thickness 1.2 m, as in Alba Pompeia and Augusta Taurinorum) was built of sequences of half a meter high fillings of round flints or river pebbles alternating to a two-storey brick level, opus mixtum (Rivoira, 1921). Many aspects of the Roman culture were inherited from the Greeks, who, in fact, utilized different sizing in brick-making during the V and IV centuries BC: from Lydian brick (in use in the ancient Lydia, in western Asia Minor) and tetradoron (60 x 60 cm, ~22 dm^3 in volume by ~40 kg) both used for private buildings, to pentadoron (75 x 75 cm, ~40 dm^3 in volume by ~70 kg) exclusively used in public edifices (Ginouvés, 1985; Hellmann, 2002), to 67 cm wide proto-Corinthian tiles approximately weighing 35 kg (Sapirstein, 2009). The nature of the clay and its original moisture is inescapably different site by site; hence also the final size of an artefact could vary (Warry, 2010). Nevertheless in about 1 AD in Rome, a fired brick was an extremely regular parallelepiped of approximately 25 kg and 8 dm^3 in volume. Its shape changed gradually along the road directed towards buildings located in northern Italian regions, i.e. combining the Etruscan influence in the measures of fired bricks (41/45 x 25/27 x 11/14 cm; Righini 1999; Bacchetta 2003), as for a simple increase in volume (12 dm^3) obtained by a simple thickening in Ravenna, Regio VIII (III BC), or deforming the whole shape (50 x 40 x 8 cm, 18 dm^3) as in Aquileja, Regio X (II BC) (Bacchetta, 2003). The Alpine area and the Po Valley have been the scene of important evolution in brick construction; here a brick longum sesquipede latum pede was similar to the 'Lydian' brick (45 x 30 cm by several cm thickness, volume ~ 6÷9 dm^3, mass ~11÷18 kg), proving the cultural relation between Western and the Eastern Mediterranean (Bruno et al., 2013; Goll, 2005; Quagliarini and Lenci, 2010). During Roman times, the measures of fired bricks were similar for both public and private buildings, including military buildings – as it was unlikely that civilian entrepreneurs have ever made bricks available to the Roman army (Kurzmann, 2005). Peculiar sizing were attributed to triangular bricks (20 x 15-20 x 8-12 cm) obtained by cutting laterculi besales – or sesquipedalians – before burning, pavements (33 x 13 x 8 cm), baths (24 x 12 x 3 cm), foundations (cutting sesquipedalians after burning) and tiles (38-77 x 28-56 cm both curved and flat) (AFBA, 1925; El-Gohary and Al-Naddaf, 2009; Giuliani, 1990). Bricks in Legio II (Heighway et al., 1982) and Legio V (measured in Potaissa castrum) or tiles (~ 2 dm^3) in Legio XX (Warry, 2010), manufactured more than 2,500 km North of Rome, were extremely similar by volume and weight (~ 5 dm^3 in volume by ~10 kg) but different in size (37 x 30 x 5 cm).

Soil accomplishes several key functions, economically and socially essential since antiquity. Actually, the most considered human function related with soil exploitation is by far production of natural goods: e.g. producing food and non-food crops. But not less important are the carrier function (*i.e.* buildings and their coupled infrastructures), the filter function (converting the quality of solutes passing through), the habitat and cultural functions and the resource function, providing base technology materials. The latter includes mining for precious metals and the direct transformation of bulk soil (van Loon, 2001). The use of land implies that some of these functions are intrinsically in competition (EC, 2006). Although the relation between land use and soil functions has been rarely refined in the course of the centuries because of technological developments (Bouma, 2006), since Roman civilization the human fingerprint on the landscape was left by a combination of soil use and an increased forest clearance (Kaplan et al., 2009). A fired brick, for instance, means a physical removal of a soil volume, its mix with a volume of water and its consequent firing, being the burning of wood the only available source of heating energy. To evaluate the amount of soil use, we must consider that a brick in Rome had a square basis one and a half Roman feet long, i.e. a sesquipedalian according to Vitruvius, corresponding to about 45 cm in length and 4 cm in height, occupying 0.008 m^3. The private building of ancient Rome at the end of the IV century AD, housing lower and middle class population, was composed of *insulae* 60 Roman feet (~18 m) wide, made of bricks and summing to more than 46,000 units in the whole Rome. In the same times the *domus*, the single-family residence of the Roman élite, were some 1,800 units (Helen, 1975). So, as an *insula* occupied some 300 m^2 by an average of six stories high (21 meters ~70 Roman feet), it results that on average as many as some 3,300 bricks were used per insula. When this amount is multiplied by the number of *insulae* and the volume occupied by one brick, it turns out into 1,200,000 m^3 of bricks. If we suppose a reduction of volume of the soil in the brick-making by 30% and a maximum depth of excavation corresponding to four meters, the area needed to provide Romans with bricks was in the order of forty hectares. This amount must be added to the remaining private and public buildings and walls existing in ancient Rome.

Approximately, just ten bricks per person, per day were reasonably realisable in Roman times. This finding is coherent with the replica experiment of very large bricks (Wolf, 2002). Apart from the labour force, brick-making used impressive quantities of fuel (in prevalence timber in Roman times) that would have probably represented up to half of the total cost of brick-making (Dobson, 1850; Warry, 2010). In the case of Rome, according to Wolf (2002) estimation of timber consumption by kiln load (12,500 kg of dry fir timber) the 150 million bricks of the capital were fired using 1.5 million m^3 of timber, which means between 1,500 and 2,000 hectares of cleared forest. In terms of soil uptake, it would correspond to a spatial ratio of 1:50 soil-raw material:forest-fuel, for the ancient brick-making.

References

AFBA (American Face Brick Association), 1925. Brickwork in Italy. American Face Brick Association, Chicago.

Bacchetta, A., 2003. Edilizia Rurale Romana. All'Insegna del Giglio Editore, Firenze [in Italian].

Bouma, J,. 2006. Soil functions and land use. In: Certini, G., Scalenghe, R. (Eds.) Soils. Basic Concepts and Future Challenges. Cambridge University Press, Cambridge, pp. 211–221.

Bruno, L., Amorosi, A., Curina, R., Severi, P., Bitelli, R., 2013. Human–landscape interactions in the Bologna area (northern Italy) during the mid–late Holocene, with focus on the Roman period. The Holocene 23, 1560–1571.

Dobson, E., 1850. A Rudimentary Treatise on the Manufacture of Bricks and Tiles. John Weale, London.

EC (European Commission), 2006. Thematic Strategy for Soil Protection. COM(2006)231 final, 22.9.2006. European Commission, Bruxelles.

El-Gohary, M.A., Al-Naddaf, M.M., 2009. Characterization of bricks used in the external casing of roman bath walls Gadara–Jordan. Mediterranean Archaeology and Archaeometry 9, 29–46.

Ginouvés, R., Martin, R., 1985. Dictionnaire Méthodique de l'Architecture Grecque et Romaine, I. Matériaux, Techniques de Construction, Technique et Forms du Décor. École Française d'Athènes, École Française de Rome, Roma [in French].

Giuliani, C.F., 1990. L'Edilizia nell'Antichità. La Nuova Italia Scientifica, Roma [in Italian].

Goll, J., 2005. Medieval brick-building in the central Alps. Archaeometry 47, 403–423.

Heighway, C.M., Parker, A.J., Goudge, C.E., Vince, A.G., Wild, F., Watkins, M.J., Bell, M., Tatton-Brown, T., Rogers, J., 1982. The Roman tilery at St Oswald's Priory, Gloucester. Britannia 13, 25–77.

Helen, T., 1975. Organization of Roman Brick Production in the First and Second Centuries AD: An Interpretation of Roman Brick Stamps. Suomalainen Tiedeakatemia, Helsinki.

Hellmann, M.C., 2002. L'Architecture Grecque. Les principes de la Construction. Picard, Paris [in French].

Kaplan, J.O., Krumhardt, K.M., Zimmermann, N., 2009. The prehistoric and preindustrial deforestation of Europe. Quaternary Science Reviews 28, 3016–3034.

Kurzmann, E., 2005. Soldier, civilian and military brick production. Oxford Journal of Archaeology 24, 405–414.

Lancaster, L.C., 2010. Parthian influence on vaulting in Roman Greece? An inquiry into technological exchange under Hadrian. American Journal of Archaeology 114, 447–472.

Quagliarini, E., Lenci, S., 2010. The influence of natural stabilizers and natural fibres on the mechanical properties of ancient Roman adobe bricks. Journal of Cultural Heritage 11, 309–314.

Righini, V., 1999. La diffusione del mattone cotto nella Gallia Cisalpina e l'architettura in mattoni di Ravenna. In: Bandala Galan, M., Rio, C., Roldan Gomez, L. (Eds.) El Ladrillo y sus Derivados en la Epoca Romana. UAM Ediciones, Madrid, pp. 125–157.

Rivoira, G.T., 1921. Architettura Romana: Costruzione e Statica nell'Età Imperiale. Ulrico Hoepli, Milano [in Italian].

Sapirstein, P., 2009. How the Corinthians manufactured their first roof tiles. Hesperia 78, 195–229.

Van Loon, A.J., 2001. Changing the face of the Earth. Earth-Science Reviews 52, 371–379.

Warry, P., 2010. Legionary tile production in Britain. Britannia 41, 127–147.

Wolf, S., 2002. Estimation of the production parameters of very large medieval bricks from St. Urban, Switzerland. Archaeometry 44, 37–65.